MERGING RADAR-ONLY QPE AND RAIN GAUGE DATA VIA CONDITIONAL BIAS-PENALIZED OPTIMAL ESTIMATION

by

BEOMGEUN KIM

Presented to the Faculty of the Graduate School of

The University of Texas at Arlington in Partial Fulfillment

of the Requirements

for the Degree of

MASTER OF SCIENCE IN CIVIL ENGINEERING

THE UNIVERSITY OF TEXAS AT ARLINGTON

December 2015

Acknowledgements

First of all, I would like to give glory to God who gave me the opportunity and strength as well as the patience to finish this work.

I really appreciate my supervising professor Dr. Dong-Jun Seo for his guidance in my academia as well as my life in U.S. It was a great pleasure to work with him and I consider myself extremely fortunate to gain this opportunity. This study would have not been possible without his valuable advices and constant feedback.

I am also thankful to Dr. Nelson and Dr. Prat of National Climate Data Center (NCDC) for their valuable contributions to this work.

I would like to express my sincere appreciation to Dr. Seong Jin Noh, Dr. Nick Z. Fang and Dr. Habib Ahmari for serving on my thesis committee. I also would like to show my sincere appreciation to Dr. Sunghee Kim for her constant help and suggestions.

I have always enjoyed working with my research lab mates as a team. Throughout my M.S. study, they have always been very kind and supported me as a friend and colleague. My special thanks go to Arezoo Rafieenasab, Hamideh Riazi, Hossein Sadeghi, Hamideh Habibi, Amir Norouzi, Behzad Nazari and recent lab mate Reza Ahmad Limon, Maurizio and Biplop Dhakal for all their love and support.

I am also thankful to my friends Rachel, Gulshot, Ken, church members and my family members who gave me a lot of advice and prayed for me to help me complete my work successfully.

November 23, 2015

Abstract

MERGING RADAR-ONLY QPE AND RAIN GAUGE DATA

VIA CONDITIONAL BIAS-PENALIZED

OPTIMAL ESTIMATION

Beomgeun Kim, MS

The University of Texas at Arlington, 2015

Supervising Professor: Dong-Jun Seo

A new technique for merging radar precipitation estimates and rain gauge data is developed and evaluated to improve multisensor quantitative precipitation estimation (QPE). Various types of linear and nonlinear techniques have been used to combine rain gauge and radar data. Linear cokriging and its variants, for example, may be considered as the best linear unbiased estimators which minimize the error variance in the unconditional sense. They are, however, subject to conditional biases (CB) that may be unacceptably large for estimation of heavy-to-extreme precipitation. In this work, I develop, apply, and evaluate conditional bias-penalized cokriging (CBPCK) for spatial estimation of precipitation using weather radar and rain gauge data which explicitly minimizes Type-II CB. The proposed CBPCK is a bivariate version of extended conditional bias-penalized kriging (ECBPK) which was developed for gauge-only estimation of heavy-to-extreme precipitation. To evaluate the proposed method, CBPCK is comparatively evaluated with a variant of ordinary cokriging (OCK), the currently used algorithm in NWS's Multisensor Precipitation Estimator (MPE), via cross validation and visual examination of merged fields. The analysis domain is about 560 x 560 km^2 in the North Central Texas region and the analysis period is from 2002 to 2011. The radar data

used is from the reanalysis of the radar-only National Mosaic and multisensor QPE (NMQ/Q2). The rain gauge data used is from the Hydrometeorological Automated Data System (HADS). The results show that CBPCK significantly reduce CB for estimation of heavy-to-extreme precipitation at subdaily scales of accumulation, and that the margin of improvement over OCK is larger when the fractional coverage of rainfall is high, i.e., when it is precipitation over most of the area over the ungauged location. CBPCK may be used in reanalysis or in real-time analysis for which accurate estimation of heavy-to-extreme precipitation is of particular importance.

Table of Contents

List of Illustrations

List of Tables

Chapter 1

Introduction

1.1. Background

Heavy-to-extreme rainfall is a growing concern since it is very often a direct cause for serious natural disasters such as flash floods, urban inundation, river floods and landslides. In recent years, weather radars have become a popular tool for quantitative precipitation estimation (QPE). Many techniques have been investigated and developed over the last 40 years for more skillful QPE with higher spatio-temporal resolution. However, radar QPE is subject to various error sources such as uncertain Z-R relationships, lack of calibration, attenuation, anomalous propagation (AP) and variations of vertical reflectivity profile (VPR), etc. (Austin, 1987; Smith et al., 1996; Steiner et al., 1999; Wilson and Brandes, 1979; Fang et al., 2004; Villarini and Krajewski, 2009). Therefore, radar-only estimates are often combined with rain gauge data, which are often considered as true precipitation, to produce more accurate QPE. Many linear and nonlinear merging techniques have been reported for multisensor QPE (e.g. Creutin et al., 1988; Delrieu et al., 2014; Goovaerts, 2000). Cokriging, for example, is one of the widely used geostatistical merging techniques (Goudenhoofdt and Delobbe, 2009; Krajewski, 1987; Seo et al., 1990a,b; Sideris et al., 2014). Its variants (Seo, 1998a,b) are currently used for radar-gauge analysis in the NWS's Multisensor Precipitation Estimator (MPE, Seo et al. 2010). Kriging, cokriging and their variants are often considered as the best linear unbiased estimators in the unconditional sense because they are unbiased and minimize error variance in the unconditional mean sense (Journel and Huibjbregts 1978). In the conditional sense, however, these optimal estimation techniques frequently underestimate large precipitation and overestimate small precipitation. This is because, to minimize error variance unconditionally, the above estimators reduce errors primarily

over the median range of precipitation amounts, which occur far more frequently (Ciach et al., 2000; Habib et al., 2013; Seo and Breidenbach, 2002). For accurate estimation specifically of large amounts, it is at least as important to reduce conditional bias (CB), in particular Type-II CB, as to minimize unconditional error variance, particularly for estimation of mean areal precipitation (MAP). Note that, in MAP estimation, random errors tend to average out whereas conditional biases do not. Type-I and Type-II CB emerge from Type-I and Type-II errors, respectively. Type-I error occurs when falsely detecting an effect which does not exist whereas Type-II error occurs when failing to detect an existing effect. Whereas Type-I CB can be reduced via calibration, Type-II CB cannot. As such, reducing Type-II CB addresses an important gap in multisensor QPE.

Toward the above end, conditional bias-penalized kriging (CBPK, Seo, 2012) has been developed for gauge-only estimation which minimizes Type-II CB in addition to unconditional error variance. More recently, extended CB-penalized kriging (ECBPK, Seo et al., 2014) has been developed to address negative estimates in areas of light precipitation. They showed that ECBPK improves estimation of heavy-to-extreme precipitation over the variant of ordinary kriging (OK), which is currently used in NWS's MPE algorithm for gauge-only analysis. Explicit minimization of CB in multisensor QPE, however, has not been investigated yet. The purpose of this work is to develop a bivariate version of ECBPK, referred to herein as conditional bias-penalized cokriging (CBPCK), and comparatively evaluate with the variant of ordinary cokriging (OCK) which is currently used in the NWS's MPE algorithm for radar-gauge analysis. Note that, while referred to as CBPCK for the sake of brevity, the proposed technique does include the enhancement made in ECBPK to address negative estimates in areas of light precipitation.

1.2. Objective

The main objective of this study is to improve multisensor estimation of heavy-to-extreme precipitation via CBPCK. Whereas the currently used MPE algorithm, a variant of OCK, minimizes unconditional error variance only (Seo, 1998 a,b), CBPCK explicitly minimizes both unconditional error variance and CB thereby improving performance for estimation of very large and very small amounts of precipitation. To evaluate CBPCK, cross validation experiments were designed and carried out over Texas. For comparison, the MPE algorithms for gauge-only and radar-gauge analyses are also carried out. To measure performance, conditional RMSE, conditional mean and multiplicative bias are used. To visual examine performance, scatter plots and quantile-quantile (QQ) plots are examined. For visual assessment of the quality of analysis, CBPCK-estimated precipitation fields are compared with precipitation fields from gauge-only, radar-only, and OCK analysis. The analysis domain is about 560 x 560 km^2 area in the North Central Texas region and the analysis period is from 2002 to 2011. The radar data used is from reanalysis of the radar-only National Mosaic and multisensor QPE (NMQ/Q2, Zhang et al., 2011). The rain gauge data used is from the Hydrometeorological Automated Data System (HADS, Kim et al., 2009).

1.3. Outline of the Thesis

This thesis is organized as follows. Chapter 1 presents the background of the study, the statement of the problem, the specific objectives of the study and the thesis organization. Chapter 2 reviews the literature on geostatistical merging techniques, CB and significant findings from relevant previous studies in precipitation estimation. Chapter 3 provides mathematical representation and description of CBPCK. Chapter 4 describes the analysis domain, the data used, and the data quality control process used. Chapter 5 describes the procedures used to estimate the statistical parameters and the assumptions used. Chapter 6 presents the results and analysis. Chapter 7 presents the conclusion and future research recommendations.

Chapter 2

Literature Review

2.1. Merging Techniques

Many geostatistical techniques have been developed to merge two or more variables in environmental science and engineering applications (e.g. Creutin et al., 1988; Delrieu et al., 2014; Goovaerts, 2000, 2000; Goudenhoofdt and Delobbe, 2009; Velasco-Forero et al., 2009). Kriging is one of the most widely used geostatistical techniques for estimation of the variable(s) of interest at unsampled locations using neighboring observations. Kriging is a so-called best linear unbiased estimator (BLUE) in the sense that it employs a linear estimator, is unbiased (unconditionally) and minimizes (unconditional) error variance. If there exist observations of auxiliary variable(s) that may be cross-correlated with those of the primary variable(s) of interest, one may use cokriging (Goudenhoofdt and Delobbe, 2009; Journel and Huijbregts, 1978; Krajewski, 1987; Seo et al., 1990a,b; Sideris et al., 2014) or similar techniques to estimate the primary variable(s) at ungauged or unsampled locations using multiple data sets. In addition to cokriging, conditional merging (Ehret, 2003), kriging with external drift (Haberlandt, 2007; Verworn and Haberlandt, 2011) and other techniques have been developed for similar purposes. Based on the mathematical form, the estimator may be linear or nonlinear, leading to linear or nonlinear estimators, respectively.

2.1.1. Nonlinear Estimation

Linear estimators are generally optimal, in the sense of BLUE, only if the variables of interest are normally distributed (i.e., multivariate normal). Precipitation , particularly short-term accumulations, has a skewed distribution. To improve estimation

of skewed variables, nonlinear cokriging methods, such as indicator cokriging and disjunctive cokriging, have been developed.

Indicator cokriging (Journel, 1983; Journel and Huijbregts, 1978; Seo, 1998a, 1996) is a nonparametric nonlinear estimation technique. The indicator variable is defined as:

$$I(u_0; z_c) = \begin{cases} 0 & if\ \ z(u_0) \leq z_c \\ 1 & if\ \ z(u_0)\ > z_c \end{cases} \tag{2.1}$$

where $I(u_0; z_c)$ denotes the indicator variable at location u_0 with the cutoff z_c (i.e., the threshold of interest), and $z(u_0)$ denotes the measurement at location u_0. Each observation can be expressed as a binary experimental outcome of 0 and 1, depending on whether it exceeds the cutoff z_c. Under the second-order homogeneity assumption, indicator cokriging can be performed at many different thresholds from which one may estimate the conditional cumulative probability distribution function (CDF) of the variable of interest at the ungauged location (Seo, 1996). The above estimation utilizes the fact that the conditional expectation of an indicator variable given the neighboring observations is equivalent to the conditional probability of the variable exceeding the threshold given the neighboring observations (see Eq.(2.1)). A variant of indicator kriging has also been used in Double Optimal Estimation (DOE, Seo, 1998b) to estimate the probability of precipitation (PoP) from rain gauge or rain gauge and radar data.

Disjunctive cokriging (Azimi-Zonooz et al., 1989; Journel and Huijbregts, 1978; Matheron, 1975; Webster and Rivoirard, 1991; Yates et al., 1986) is a parametric version of indicator cokriging. It transforms each variable into a normal deviate via the Hermite polynomial transformation (Journel and Huijbgregts 1978), assumes multivariate normality of the transformed variables, performs estimation in the normal space, and back-transforms the estimate and estimation variance into the original space. For real-

time estimation, however, disjunctive kriging may not very desirable for computational cost and the fact that, unlike indicator kriging, it is not suited to handle the discrete probability mass at zero for no precipitation.

2.1.2. Linear Estimation Using Multiple Variables

Simple and ordinary cokriging are widely used geostatistical techniques when two or more variables are available. When the gauge observations of precipitation and radar estimates of precipitation are jointly second-order homogeneous, ordinary or simple cokriging may be used. Simple cokriging (SCK) may be used when the mean of gauge precipitation is known from an independent source of information. If rain gauge observations and radar data are the primary and secondary variables, respectively, the SCK estimator is made of the known mean and the linear weighted combination of the residuals as shown below:

$$G_k^*(u_0) = m + \sum_{i=1}^{n_g} \lambda_{gi} \left[G_k(u_i) - m\right] + \sum_{j=1}^{n_r} \lambda_{rj} \left[R_k(u_j) - m\right] \quad (2.2)$$

where $G_k^*(u_0)$ denotes the estimated precipitation at the ungauged bin centered at u_0 in hour k, m is the known spatially-constant mean precipitation, $G_k(u_i)$ denotes the gauge precipitation at location u_i at hour k, $R_k(u_j)$ denotes the radar precipitation at location u_j at hour k, λ_{gi} denotes the weights given to the i-th gauge observation, n_g denotes the number of the nearest gauges used, and the subscripts g and r signify that the variables are associated with gauge-observed and radar-estimated precipitation, respectively. The optimal weights, λ_{gi} and λ_{rj} in Eq.(2.2), are obtained by minimizing the error variance:

$$Var[G_k(u_0) - G_k^*(u_0)] = E[\{G_k(u_0) - G_k^*(u_0)\}^2] \quad (2.3)$$

Ordinary cokriging (OCK) may be used when there is no prior knowledge available about the mean of gauge-observed precipitation and the mean of radar–estimated precipitation. The OCK estimator is expressed as:

$$G_k^*(u_0) = \sum_{i=1}^{n_g} \lambda_{gi}\, G_k(u_i) + \sum_{j=1}^{n_r} \lambda_{rj}\, R_k(u_j) \quad (2.4)$$

$$\sum_{i=1}^{n_g} \lambda_{gi} + \sum_{j=1}^{n_r} \lambda_{rj} = 1 \quad (2.5)$$

where the sum of the weights, λ_{gi} and λ_{rj}, is equal to unity to force unbiasedness, which may be easily verified by taking expectations on both sides of Eq.(2.4) and applying Eq.(2.5). The weights, λ_{gi} and λ_{rj} in Eq.(2.4), are obtained by minimizing the unconditional error variance. Though cokriging has been widely used, the original formulations do not address intermittency of precipitation. To address precipitation intermittency and inner variability explicitly, Single Optimal Estimation (SOE) and Double Optimal Estimation (DOE) were developed (Seo, 1998 a,b) which are used in MPE (Seo et al. 2010).

2.2. Conditional Bias (CB)

Kriging or its variants provide unbiased precipitation estimates as well as minimum error variance in the unconditional sense. In the conditional sense, however, these optimal estimation techniques tend to overestimate light precipitation and underestimate heavy precipitation (Ciach et al., 2000; Seo, 2012b; Seo et al., 2014). These tendencies arise because the number of precipitation observations near the median is necessarily much larger than those over the tails. To minimize unconditional error variance, the BLUE estimators improve accuracy around the median, where precipitation occurs very frequently, rather than over the tails, where precipitation occurs very infrequently. For accurate estimation specifically of large amounts, however, it is very important to reduce CB, in particular Type-II CB, than to minimize unconditional error variance.

Type-I and Type-II CB emerge from Type-I and Type-II errors, respectively. Type-I error is associated with a false alarm (e.g. crying wolf without a wolf in sight), while

Type-II error is associated with failing to raise an alarm (i.e. failing to see the wolf). Type-I CB is defined as $\mathrm{E}\left[X\middle|\hat{X}=\hat{x}\right]-\hat{x}$ where X, $\hat{X}$, and $\hat{x}$ denote the unknown truth, the estimate and the realization of $\hat{X}$, respectively (Jolliffe and Stephenson, 2012). Type-I CB exists when, given the estimate, the expected value of the unknown truth is different from the realization of the estimate. Type-II CB is defined as $\mathrm{E}\left[\hat{X}\middle|X=x\right]-x$ where X, $\hat{X}$, and x denote the unknown truth, the estimate and the realization of X, respectively. Type-II CB exists when, given the unknown truth, the expected value of the estimate is different from the realization of the unknown truth. Whereas Type-I CB can be reduced by calibration (e.g., If the false alarm rate is too high, one may not cry wolf as often), Type-II CB is not amenable to statistical bias correction or post processing (Brown and Seo, 2013). Throughout the rest of this thesis, Type-II CB is referred to as CB for brevity.

Seo (2012) developed CBPK which minimizes both unconditional error variance and CB of the estimate. The resulting CBPK system is a very simple extension of the simple kriging (SK) system and can be implemented very easily in an existing SK or OK code. Brown and Seo (2012) have proposed a nonparametric technique to minimize Type-II CB in streamflow prediction. This technique is analogous to indicator cokriging (ICK) and is referred to as conditional bias-penalized indicator cokriging (CBP-ICK). They showed that CBP-ICK successfully reduces Type-II CB and produces more skillful estimates than the estimates from other post-processing techniques used in hydrologic prediction.

Because CBPK minimizes both unconditional error variance and conditional CB, its solution is not as good as OK's in the unconditional sense. As such, the CBPK estimates are inferior to the OK estimates around the median and superior over the tails. If one can predict, with a high degree of accuracy, the general range of the truth by utilizing soft information that may be available, one may use both CBPK and OK

depending on the a priori determination of the magnitude of the truth. Toward that end, this work develops, applies and evaluates a bivariate version of ECBPK (Seo et al. 2014), referred to as CBPCK, which combines CBPK and the bivariate version of OK for spatial estimation of precipitation using radar QPE and rain gauge observations.

Chapter 3

Methodology

In this section, two different merging techniques are described: (1) the bivariate version of OCK used in Multisensor Precipitation Estimator (MPE, Seo et al. 2010) in NWS; and (2) the bivariate version of ECBPK (Seo et al., 2014).

3.1. Ordinary Cokriging (OCK)

OCK estimates the precipitation amount at an ungauged location given the neighboring rain gauge observations and the radar QPE. The OCK estimator has the following form:

$$G_k^*(u_0) = \sum_{i=1}^{n_g} \lambda_{gi}\, G_k(u_i) + \sum_{j=1}^{n_r} \lambda_{rj}\, R_k(u_j) \tag{3.1}$$

$$\sum_{i=1}^{n_g} \lambda_{gi} + \sum_{j=1}^{n_r} \lambda_{rj} = 1 \tag{3.2}$$

where $G_k^*(u_0)$ denotes the estimated precipitation at the ungauged bin centered at u_0 in hour k, $G_k(u_i)$ and $R_k(u_j)$ denote gauge and radar precipitation at location u_i in hour k, respectively, λ_{gi} and λ_{rj} denotes the weights given to the i-th gauge and the j-th radar data ,respectively, n_g and n_r denote the number of gauge and radar used ,respectively. The constraint, Eq.(3.2), renders the estimate $G_k^*(u_0)$ in Eq.(3.1) unbiased in the mean sense. The weights given to the nearest gauge and radar data, λ_{gi} and λ_{rj} in Eq.(3.1), respectively, are obtained by minimizing the error variance of $G_k^*(u_0)$ (see Seo, 1998b for details). The above formulation assumes that the radar precipitation estimates, $R_k(u_j)$, are unbiased.

The optimal weights, λ_{gi} and λ_{rj} , can be obtained by minimizing the error variance of the estimate, J_{OCK}:

$$J_{OCK} = Var[G_k^*(u_0) - G_k(u_0)] = E[\{G_k^*(u_0) - G_k(u_0)\}^2] = 1 - \sum_{i=1}^{n_g+n_r} \lambda_i\, \rho_{i0} - \mu \tag{3.3}$$

where μ denotes the Lagrange multiplier (Journel and Huijbregts, 1978). The optimal weights are a function of the covariances of gauge and radar precipitation and the cross-covariance between the two. The covariance, e.g., is given by (Seo, 1998a,b):

$$\mathrm{Cov}\left[\mathrm{G}(u_i), R(u_j)\right] = E[G(u_i) \cdot R(u_i)] - E[G(u_i)] \cdot E[R(u_i)]$$

$$= E\left[G(u_i) \cdot R(u_i) | G(u_i) > 0, R(u_j) > 0\right] \cdot \Pr\left[G(u_i) > 0, R(u_j) > 0\right]$$

$$- \mathrm{E}[G(u_i) | G(u_i) > 0] \cdot \Pr[G(u_i) > 0] \cdot \mathrm{E}\left[R(u_j) \middle| R(u_j) > 0\right] \cdot \Pr[R(u_j) > 0] \quad (3.4)$$

In the above, the time index k is dropped for notational brevity. Eq.(3.4) can be rewritten as:

$$\mathrm{Cov}\left[\mathrm{G}(\mathrm{u_i}), \mathrm{R}(\mathrm{u_j})\right] = \sigma_g \sigma_r \left[\mathrm{m_{Ig}}(1 - \mathrm{m_{Ig}})\right]^{\frac{1}{2}} [\mathrm{m_{Ir}}(1 - \mathrm{m_{Ir}})]^{\frac{1}{2}} \rho_c(|\mathrm{u_i} - \mathrm{u_j}|) \rho_{\mathrm{Ic}}(|\mathrm{u_i} - \mathrm{u_j}|)$$

$$+ \mathrm{m}_g \mathrm{m}_r [\mathrm{m_{Ig}}(1 - \mathrm{m_{Ig}})]^{1/2} [\mathrm{m_{Ir}}(1 - \mathrm{m_{Ir}})]^{1/2} \rho_{Ic}(|\mathrm{u_i} - \mathrm{u_j}|) + \sigma_g \sigma_r \mathrm{m_{Ig}} \mathrm{m_{Ir}} \rho_c(|\mathrm{u_i} - \mathrm{u_j}|) \quad (3.5)$$

where σ_g and σ_r denotes the standard deviation of gauge and radar precipitation, respectively, $\mathrm{m_{Ig}}$ and $\mathrm{m_{Ir}}$ denote the mean fractional coverage by rain gauge and radar precipitation, respectively, m_g and m_r denote the unconditional mean of gauge and radar precipitation, respectively, and $\rho_c(|\mathrm{u_i} - \mathrm{u_j}|)$ and $\rho_{\mathrm{Ic}}(|\mathrm{u_i} - \mathrm{u_j}|)$ denote the conditional and indicator cross-correlation functions between gauge and radar precipitation, respectively. Under the assumption of homogeneity, the mean fractional coverage of precipitation is equivalent to PoP (Seo and Smith, 1996). As in Seo (1998b), it is assumed in Eq.(3.5) that σ_g is the same as σ_r, $\mathrm{m_{Ig}}$ is the same as $\mathrm{m_{Ir}}$, $\rho_c(|\mathrm{u_i} - \mathrm{u_j}|)$ is the same as $\rho_{\mathrm{Ic}}(|\mathrm{u_i} - \mathrm{u_j}|)$ and m_g is the same as m_r. These assumptions reduce Eq.(3.5) to:

$$\mathrm{Cov}\left[\mathrm{G}(\mathrm{u_i}), \mathrm{R}(\mathrm{u_j})\right] = \sigma_r^2 \cdot [\mathrm{m_{Ir}}(1 - \mathrm{m_{Ir}})] \cdot \rho_c(|\mathrm{u_i} - \mathrm{u_j}|) \cdot \rho_{\mathrm{Ic}}(|\mathrm{u_i} - \mathrm{u_j}|) + \mathrm{m}_r^2 \cdot [\mathrm{m_{Ir}}(1 - \mathrm{m_{Ir}})] \cdot$$

$$\rho_{\mathrm{Ic}}(|\mathrm{u_i} - \mathrm{u_j}|) + \sigma_r^2 \cdot \mathrm{m}_{\mathrm{Ir}}^2 \cdot \rho_c(|\mathrm{u_i} - \mathrm{u_j}|) \quad (3.6)$$

If our interest is only in the estimate and not in the estimation variance, OK may be performed using correlation instead of covariance. Dividing Eq.(3.6) with the variance of

radar precipitation, $\mathrm{Var}[\mathrm{R}(u)] = \sigma_r^2 \cdot \mathrm{m_{Ir}} + \mathrm{m}_r^2 \cdot \mathrm{m_{Ir}}(1 - \mathrm{m_{Ir}})$, results in the correlation between $G(u_i)$ and $R(u_j)$:

$$\mathrm{Corr}\left[\mathrm{G}(\mathrm{u_i}), \mathrm{R}\left(\mathrm{u_j}\right)\right] =$$

$$\frac{\mathrm{CV}_r^2 \cdot (1-\mathrm{m_{Ir}}) \cdot \rho_c(|\mathrm{u_i}-\mathrm{u_j}|) \cdot \rho_{\mathrm{Ic}}(|\mathrm{u_i}-\mathrm{u_j}|) + (1-\mathrm{m_{Ir}}) \cdot \rho_{\mathrm{Ic}}(|\mathrm{u_i}-\mathrm{u_j}|) + \mathrm{CV}_r^2 \cdot \mathrm{m_{Ir}} \cdot \rho_c(|\mathrm{u_i}-\mathrm{u_j}|)}{\mathrm{CV}_r^2 + (1-\mathrm{m_{Ir}})} \tag{3.7}$$

where CV_r denotes the coefficient of variation (CV) of radar precipitation. The optimal weights in Eqs.(3.1) and (3.2) are obtained by solving the so-called kriging system (Journel and Huijbregts, 1978):

$$\begin{bmatrix} C_{GG} & C_{GR} & 1 \\ C_{RG} & C_{RR} & \vdots \\ 1 \;\; \ldots & 1 & 0 \end{bmatrix} \begin{bmatrix} \lambda_{\mathrm{i}} \\ \vdots \\ \lambda_{\mathrm{i+j}} \\ \mu \end{bmatrix} = \begin{bmatrix} C_{0G} \\ C_{0R} \\ 1 \end{bmatrix} \tag{3.8}$$

where C_{GG}, C_{GR} (=C_{RG}^T), and C_{RR} denotes (n_g) x (n_g), (n_g) x (n_r), (n_r) x (n_r) covariance matrices whose entries are given by $\mathrm{Cov}[\mathrm{G}(\mathrm{u_i}), \mathrm{G}(\mathrm{u}_i)]$, $\mathrm{Cov}\left[\mathrm{G}(\mathrm{u_i}), \mathrm{R}\left(\mathrm{u}_j\right)\right]$ and $\mathrm{Cov}\left[R\left(\mathrm{u}_j\right), \mathrm{R}\left(\mathrm{u}_j\right)\right]$, respectively, and C_{0G} and C_{0R} are the (1) x (n_g) and (1) x (n_r) covariance vector whose entries are given by $\mathrm{Cov}[\mathrm{G}(\mathrm{u_0}), \mathrm{G}(\mathrm{u}_i)]$ and $\mathrm{Cov}\left[\mathrm{G}(\mathrm{u_0}), \mathrm{R}\left(\mathrm{u_j}\right)\right]$, respectively $(\mathrm{i} = 1, \ldots, n_g, \mathrm{j} = 1, \ldots, n_r)$.

3.2. Conditional Bias-Penalized Cokriging (CBPCK)

CBPCK is the bivariate version of ECBPK (Seo et al., 2014). In CBPCK, the CB penalty term $E[\{E[G^*(u_0)|G(u_0)] - G(u_0)\}^2]$ is added to the objective function where the time index k has been dropped for notational brevity:

$$J_{CBPCK} = E[\{G^*(u_0) - G(u_0)\}^2] \; + \alpha \bullet E[\{E[G^*(u_0)|G(u_0)] - G(u_0)\}^2] \tag{3.9}$$

where α denotes the positive weight given to the CB penalty term. The weight, α, can be optimized to improve the balance between reducing error variance and reducing CB. If α is zero, J_{CBPCK} is the same as J_{OCK} described in Section 3.1. To specify $E[G^*(u_0)|G(u_0)]$ in

Eq.(3.9), the Bayesian optimal estimator (Schweppe, 1973) is used. The CBPCK system then results from minimizing J_{CBPCK} in Eq.(3.9) with respect to the weights, $\lambda_i's$, below:

$$\sum_{j=1}^{n_g+n_r} \lambda_j \left(\rho_{ij} + \alpha \cdot \rho_{i0} \cdot \rho_{j0}\right)\sigma_i \cdot \sigma_j = (1+\alpha)\rho_{i0} \cdot \sigma_i \cdot \sigma_0 \quad i = 1, \dots, n_g + n_r \tag{3.10}$$

$$\sum_{i=1}^{n_g} \lambda_{gi} + \sum_{j=1}^{n_r} \lambda_{rj} = 1 \tag{3.11}$$

where ρ_{ij} denotes the correlation between the two variables.

3.2.1. Fractional Coverage-Dependent Long-Term Bias Correction

CBPK often produce negative estimates in areas of light precipitation. To address this, the bias correction procedure in ECBPK (Seo at el. 2014) has been applied to CBPCK in which the negative CBPCK estimates set to be zero and the scaling coefficient, γ, is applied to the positive CBPCK estimates:

$$G^*(u_0)'_{CBPCK} = \begin{cases} 0 & if \;\; G^*(u_0)_{CBPCK} < 0 \\ \gamma \cdot G^*(u_0)_{CBPCK} & otherwise \end{cases} \tag{3.12}$$

Where $G^*(u_0)'_{CBPCK}$ denotes the bias-corrected CBCPK estimates and the scaling coefficient, γ, is empirically estimated as a function of the fractional coverage of precipitation over the ungauged location by:

$$\gamma = \frac{E[G^*(u_0)_{CBPCK}]}{E[G^*(u_0)_{CBPCK} | G^*(u_0)_{CBPCK} > 0]} \tag{3.13}$$

where $E[G^*(u_0)_{CBPCK}]$ denotes the spatiotemporal mean of CBPCK estimate, $G^*(u_0)$, at location u_0 and $E[G^*(u_0)_{CBPCK} | G^*(u_0)_{CBPCK} > 0]$ denotes the spatiotemporal mean of positive CBPCK estimate, $G^*(u_0)$. The scaling coefficient, γ, is estimated for each subrange of the fractional coverage of precipitation. The fractional coverage is calculated by dividing the number of neighboring positive observations by the total number of neighboring observations. If there are no gauge data within the radius of influence, the fractional coverage is estimated by using the radar data only, whereas, if no radar data

exist within the radius of influence, only the rain gauge data are used to estimate the fractional coverage. If both gauges and radar report precipitation somewhere in the radius of influence, the fractional coverage is estimated via arithmetic averaging of the two.

3.2.2. Co-utilizing OCK and CBPCK

While CBPK is superior to OK over the tail ends of the distribution, it is inferior over the mid-ranges (Seo, 2012). The aim of co-utilizing OCK and CBPCK is to choose one of the two based on the most skillful information available about the magnitude of the true precipitation. In reality, however, we do not know what the true precipitation amount is at the ungauged location. In the absence of any other sources of information, one might consider the radar QPE as the best guess for true precipitation. Radar QPE, however, is generally biased in distribution relative to rain gauge observations. One might also consider the nearest rain gauge observation, but it very quickly loses skill if the distance increases. The OCK estimate, on the other hand, reflects precipitation information in both rain gauge and radar data. As such, the OCK estimate is considered as the most skillful in this work and transformed into the standard normal deviate, Z_{OCK}, which then specifies the weight alpha given to CB term, α, through a simple functional relationship. The decided relationships between alpha and Z_{OCK} are $\alpha=f(Z)=0.5Z_{OCK}^2$ for the analysis period from 2002 to 2008 and $\alpha=f(Z)=0.286Z_{OCK}^2$ for the analysis period from 2008 to 2011 by conducting sensitivity analysis. As a result, in the mid-ranges, alpha is smaller and hence the final estimate is closer to the OCK estimate, whereas, in the tails alpha is larger and hence the final estimate is closer to the CBPCK estimate.

Chapter 4

Analysis Domain and Data Acquisition

4.1. Analysis Domain

The analysis domain is the North Central Texas region as shown in Figure 4.1. The climate of the domain is humid-subtropical with hot summers and relatively mild winters. Summer daytime temperatures frequently exceed 100°F. Average high and low temperatures range from 37°F in January to 98°F in August. Mean annual precipitation also varies considerably, ranging from less than 20 inches to the West to more than 50 inches to the East.

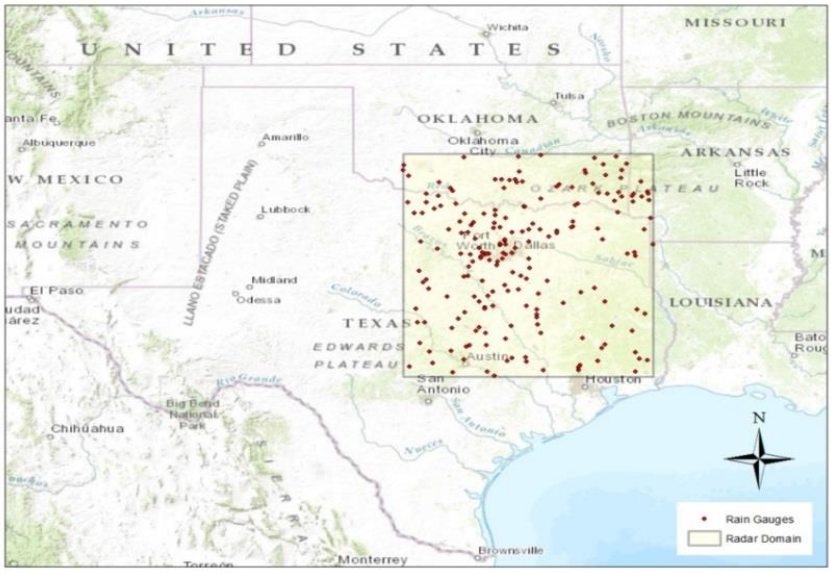

Figure 4.1 Analysis domain.

4.2. Rain Gauge Data

The rain gauge data used is from HADS which is operated by the NWS Office of Hydrologic Development (OHD, now the National Water Center). The data come from more than 10,000 rain gauges across the Continental U.S. (CONUS). A total of 199 rain gauges out of 243 are chosen through quality control process within the analysis domain.

4.3. Radar Data

The radar data used is the reanalysis at the National Clmatic Data Center (NCDC, Heiss et al., 1990) of the radar-only National Mosaic and multisensor QPE (NMQ/Q2) for which the primary source is the NEXt generation RADar (NEXRAD, Heiss et al., 1990). NMQ incorporates data from different observing systems to create high-resolution national multisensor QPE for various applications such as flash flood and flood warnings and water resources management. The main capability for QPE in the NMQ system (Zhang et al., 2011) is the next generation QPE, or Q2 (Vasiloff et al., 2007). Q2 generates multiple products such as radar-only QPE, local bias-corrected radar QPE, gauge-only QPE, and Q2 Mountain Mapper (MM), etc. The NMQ/Q2 products have been evaluated over the twelve River Forecast Center (RFC) service areas in CONUS using rain gauge observations from the Automated Surface Observing System (ASOS) (Wu et al., 2011). The results indicate that the radar-only QPE from Q2 have higher correlation and lower bias compared to those from the WSR-88D Precipitation Processing Subsystem (PPS, Fulton et al., 1998). In this work, hourly radar-only NMQ/Q2 for the 10-year period of 2002 to 2011 is used. The radar data is on a 502 × 502 grid over the analysis domain with a spatial resolution of 0.01° × 0.01°. The upper-left corner of the analysis domain is 35.01 °N latitude and 99.00 °W longitude. Table 1 summarizes the rain gauge and radar data used in this work.

Table 4.1 Data used

	Spatial Resolution	Temporal Resolution	Analysis Period	Source
Radar data	0.01° × 0.01°	1 hour	2002 - 2011	NOAA/NCDC
Rain gauge data	point	1 hour	2002 - 2011	NOAA/NCDC

4.4. Quality Control (QC) of Rain Gauge Data

Rain gauge observations are subject to systematic biases (Essery and Wilcock, 1990; Fankhauser, 1998; Sevruk et al., 1991) and have numerous sources of error such as wind, mechanical malfunction, electronic malfunction, biological contamination, etc. This subsection describes how the rain gauge data were quality-controlled before being used in multisensor QPE in this work.

4.4.1. Range Check

Figure 4.2 shows the 100-year return period for hourly precipitation in the Texas region. Based on the map, a cap of 125 mm/hr was set for hourly gauge observations. A few data points exceeded this threshold. They were then compared with the neighboring gauge observations, determined to be outliers and thrown out.

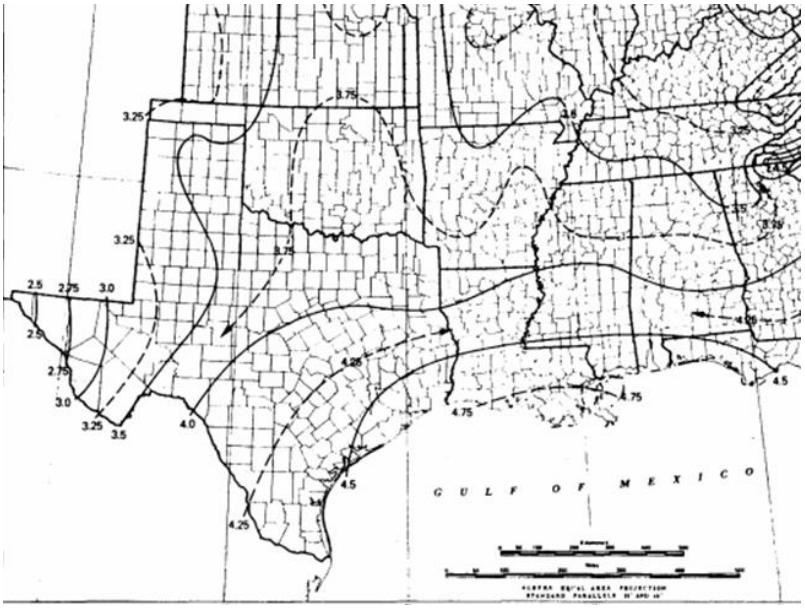

Figure 4.2 100-year 1-hour precipitation (in inches) in Texas and vicinity (Frederick et al., 1977).

4.4.2. Summary-Statistical Check

To quality control individual rain gauges, PoP and the conditional (on positive precipitation) coefficient of variation (CV) of hourly gauge precipitation are calculated for each gauge for the entire period of record (Seo and Breidenbach 2002). PoP is calculated by the number of positive gauge reports divided by the total number of gauge reports. The conditional CV is the conditional standard variation divided by the conditional mean. If the PoP or the conditional CV of the rain gauge precipitation is too large or too small compared to the reginal climatology represented by the general pattern of the statistics, the gauge is considered suspect and discarded. Figure 4.3 shows the PoP and conditional CV of hourly rain gauge precipitation at the 199 locations after throwing out suspicious gauge locations.

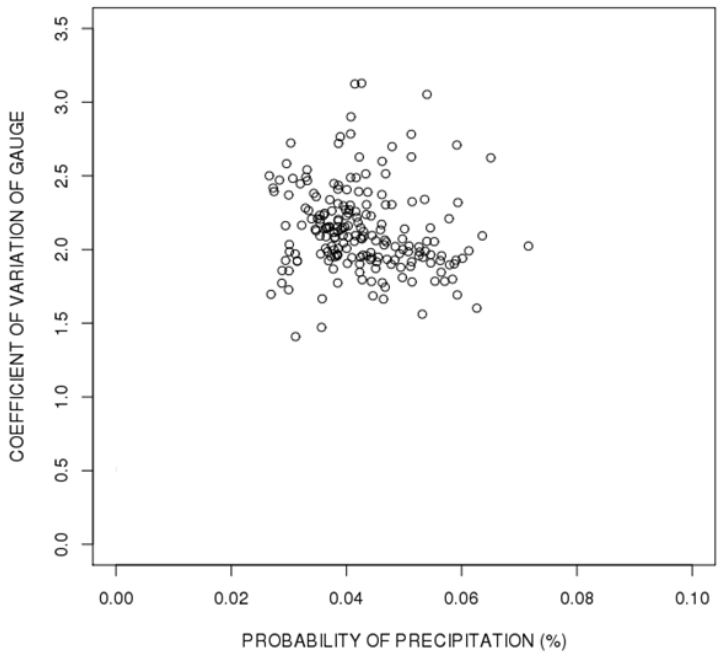

Figure 4.3 Probability of precipitation and coefficient of variation of 199 rain gauge locations within the analysis domain after removing suspicious gauges.

4.4.3. Gauge-Radar Comparison

Gauge-radar comparisons are useful in screening out malfunctioning rain gauges as well as highly suspect individual rain gauge reports. For example, if a gauge continuously reports no precipitation while radar continuously reports positive precipitation in a non-ground clutter zone, the gauge is identified as malfunctioning and thrown out. The rain gauge data are visually inspected extensively against radar QPE for quality control. For example, if the gauge data show little or no patterns of correlation with radar data in scatter plots, the gauge is thrown out. To use as much data as possible, the scatter plots are generated on monthly, seasonal and annual bases so that, if a gauge is identified as stuck for a certain period, only the data in the impacted period is excluded while the rest is retained. In addition, unusually large rain gauge observations are compared with neighboring gauge and radar data to exclude unrealistic data points. Other statistics, such as the unconditional and conditional mean of gauge and radar precipitation, the ratio of the sum of gauge precipitation to the sum of radar precipitation and the indicator and conditional correlation coefficients between gauge and radar precipitation are also examined to aid the above analysis.

Chapter 5

Estimation of Statistical Parameters

5.1. Correlation Structure Analysis

The merging algorithms used in this work require modeling spatial covariance structures of intermittency and inner variability of precipitation (Seo, 1998a,b). Because it is impractically difficult to estimate time-varying covariance structures due to lack of data and large computing requirements, climatological correlograms from the 7-year period of 2002 to 2008 are used. In this work, the correlogram structures are estimated using the hourly radar QPE under the assumption that the correlogram structures of gauge precipitation are the same as that of radar precipiation (Seo, 1998b). The conditional and indicator correlograms are estimated for each month. The experimental correlograms of radar QPE are estimated first, and then they are fitted with the exponential, Gaussian, and spherical models with the nugget effect, sill and range as the model paramters (Journel and Huijbregts, 1978). In almost all cases, both the conditional and indicator correlograms are fitted very well with the exponential model. As such, the experimental model was used throughout all analyses.

Figure 5.1 shows examples of the fitted conditional and indicator correlograms. In each panel, the dotted line represents the experimental correlogram and the solid line represents the fitted correlogram model.

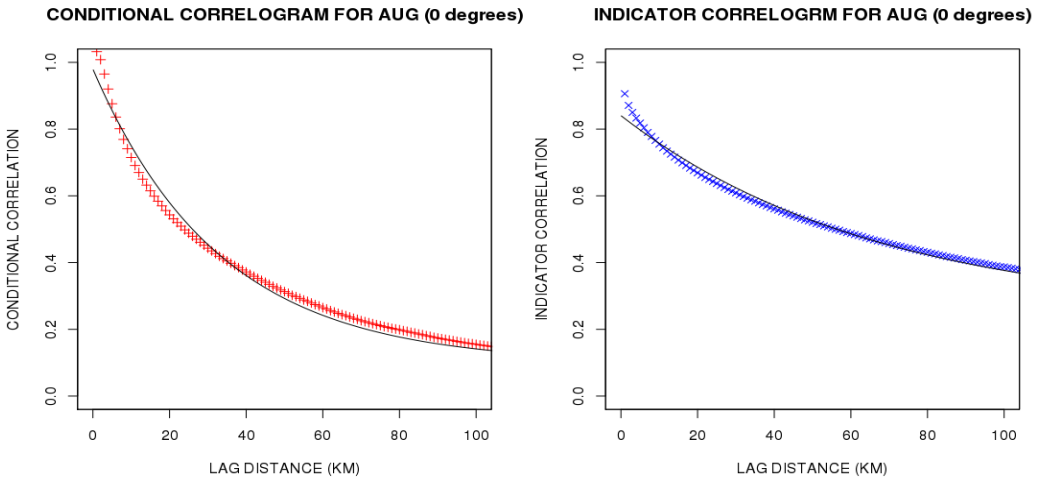

Figure 5.1 Examples of fitted conditional (left) and indicator (right) correlograms along 0 degree (i.e. horizontal line) for August.

In reality, precipitation fields are generally anisotropic. To determine anisotropy, directional experimental correlograms are calculated along the angles of 0°, 26.6°, 45°, 63.4°, 90°, 116.6°, 135°, and 153.4° counterclockwise from due east. Each experimental correlogram is then fitted with the exponential, Gaussian, and spherical models.

Figure 5.2 shows the conditional and indicator correlation structures along the eight directions for August and November. If the directional correlograms are close to one another such as in August, the precipitation fields are generally isotropic whereas, if the correlograms are different from one another, they are anisotropic. The isotropic structure is generally associated with the convective precipitation in the warm season, whereas the anisotropic structure is usually associated with the frontal precipitation in the cool season. Figure 5.3 presents the contour plots of the conditional and indicator correlograms for August and November which show more clearly about the correlation structures and their seasonal variations. Examination of the above results for all months indicates that anisotropy is not very strong in the wettest month in June for the analysis period. As such,

even though anisotropy is observed in the less-wet cool season, anisotropy is assumed in this work.

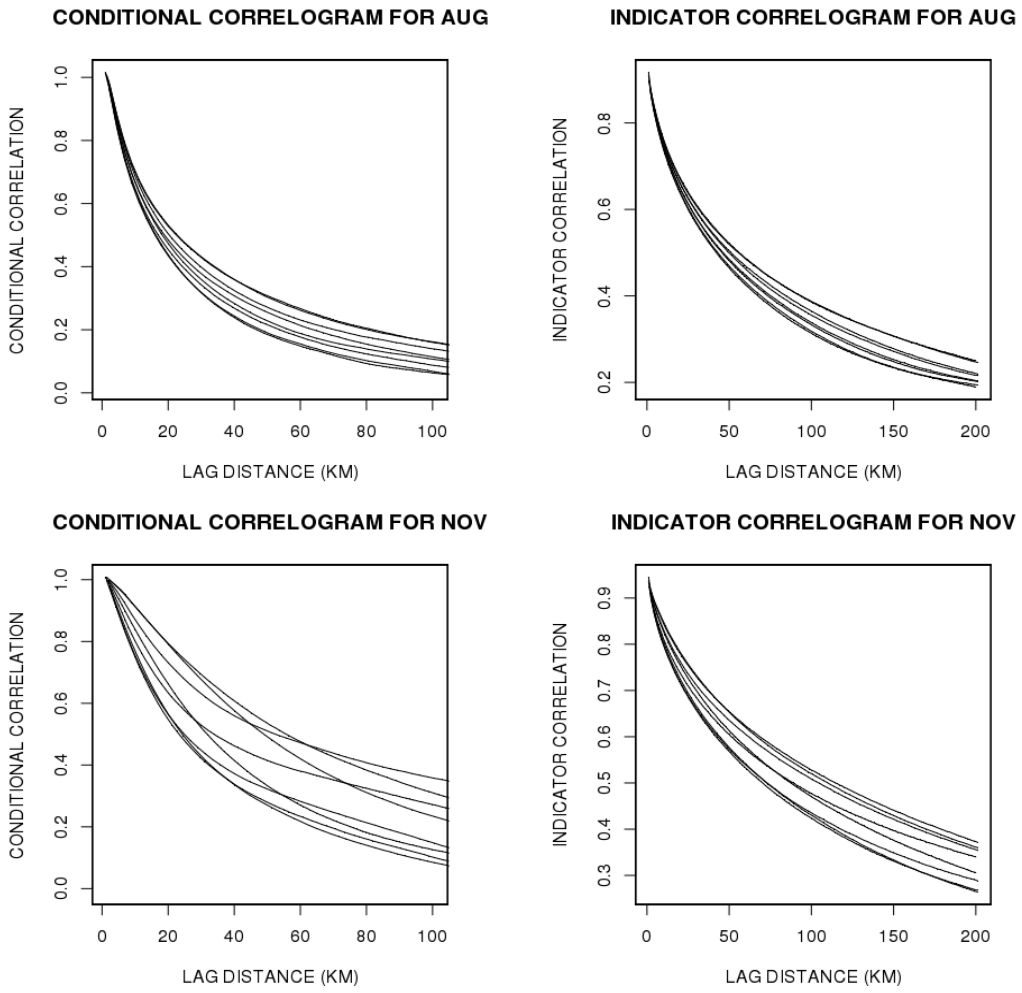

Figure 5.2 Conditional (left) and indicator (right) correlograms along the eight directions (0°, 26.6°, 45°, 63.4°, 90°, 116.6°, 135°, and 153.4°) for August (upper) and November (lower).

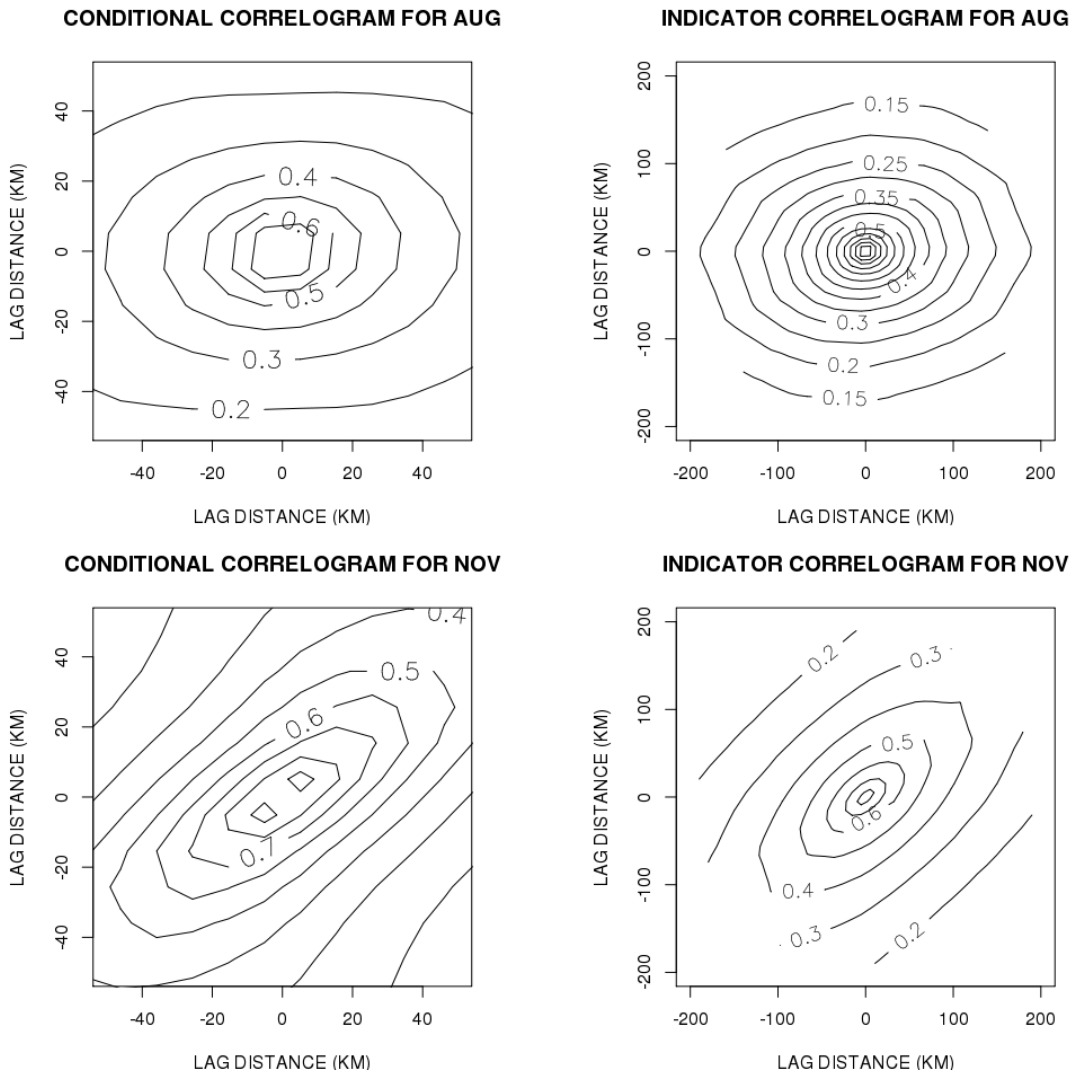

Figure 5.3 Contour plots of conditional and indicator correlograms for August (upper) and November (below).

Table 5.1 and Table 5.2 show the conditional correlogram model and indicator correlogram model, respectively, for each month.

Table 5.1 Conditional correlogram model for each month

MONTH	MODEL	RELATIVE NUGGET EFFECT	RANGE (KM)		
			AVERAGE	MINIMUM	MAXIMUM
JAN	ex	0.03	51.3	38.1	81.7
FEB	ex	0.03	47.4	31.9	71.3
MAR	ex	0.01	42.8	30.6	63.5
APR	ex	0	58.9	33.8	127.2
MAY	ex	0	43.2	31.9	60.1
JUN	ex	0	36	29.4	45.5
JUL	ex	0.01	27.1	23	34
AUG	ex	0.01	27.6	24.2	33
SEP	ex	0.01	38.6	35.3	42.5
OCT	ex	0	59	40.3	81.7
NOV	ex	0	52.4	30.3	98.3
DEC	ex	0.04	43.2	31.5	68.4

* ex: exponential

Table 5.2 Indicator correlogram model for each month

MONTH	MODEL	RELATIVE NUGGET EFFECT	RANGE (KM)		
			AVERAGE	MINIMUM	MAXIMUM
JAN	ex	0.17	97.5	85.2	105.5
FEB	ex	0.15	94.9	82.7	107.9
MAR	ex	0.16	92.5	84.3	101.2
APR	ex	0.15	97.4	91.2	105.6
MAY	ex	0.15	96.7	91.7	101.5
JUN	ex	0.19	82.5	78.1	88.2
JUL	ex	0.22	57.3	54.7	59
AUG	ex	0.21	66.2	60.3	70.6
SEP	ex	0.19	70.5	65.3	74
OCT	ex	0.16	97.2	91.4	101.4
NOV	ex	0.16	81.4	73.6	88.9
DEC	ex	0.18	94.3	86.8	103.9

* ex: exponential

The radius of influence for the neighboring observations is specified by the indicator correlation scale. The fractional coverage of precipitation within the radius of influence, m_{Ir} in Eq.(3.7), is specified dynamically from real-time observations of rain gauge and radar data by dividing the number of neighboring positive precipitation-reporting observations by the total number of neighboring observations that include zero precipitation. If both data sources are not available within the radius of influence, the fractional coverage is estimated by using only a single source. The number of neighbors used in the estimation process is 30, as determined from sensitivity analysis. The actual number of rain gauges used, however, may vary from hour to hour because only the rain gauges inside the radius of influence are used in the estimation process. Figure 5.4 shows the histogram of the actual number of gauge observations used in the analysis period of 2002 through 2008.

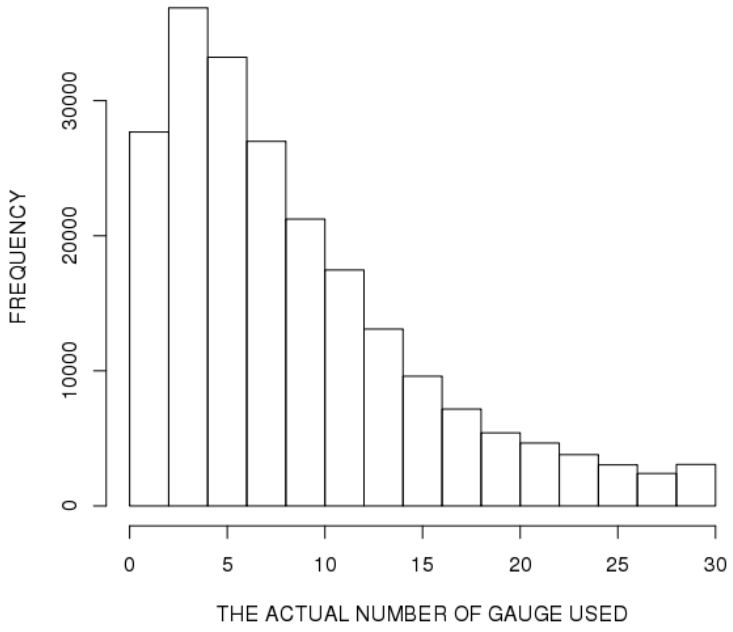

Figure 5.4 The frequency of the actual number of gauge used for cross validation (2002-2008).

Chapter 6

Results and Analysis

6.1. Cross Validation

Cross validation was performed using hourly radar QPE and hourly rain gauge observations to evaluate the proposed technique. The process of cross validation includes the following steps: 1) withhold hourly rain gauge observations one at a time and estimate precipitation at the withheld gauge location using all available data except the withheld rain gauge measurement; 2) compare the estimated amount against the withheld rain gauge measurement; 3) repeat the first and second steps for all rain gauge locations in the entire cross-validation period. Cross validation is performed for OCK, CBPCK, gauge-only and radar-only QPE. The gauge-only estimates and the radar-only estimates are denoted as GO and RO below, respectively.

6.1.1. Scatter Plots and Quantile-Quantile (QQ) plots

Figure 6.1 shows the scatter and QQ (in red) plots of the GO, RO, OCK and CBPCK estimates vs. the hourly gauge precipitation. Note that GO (upper-left) and OCK (lower-left) tend to significantly underestimate large precipitation amounts (>50mm). RO is reasonably conditionally unbiased in the global sense but generally have a larger scatter compared to OCK and CBPCK. Figure 6.2 is the same as Figure 6.1 but only for those data points for which the estimated fractional coverage (FC) over the ungauged location is greater than 0.9 (i.e., it is precipitating in most of the local area). Note that CBPCK significantly improves over both RO and OCK, greatly improves estimation of large precipitation amounts over OCK, but overestimates a large number of smaller amounts compared to OCK and a small number of smaller amounts compared to RO. The isolated significant overestimation of smaller amounts by CBPCK compared to RO

due to overestimation in the standard normal space by OCK as explained below. Recall that the weight alpha, α, for the CB term in CBPCK is specified by the standard normal transform of the OCK estimate. If OCK incorrectly overestimates small amounts, the OCK estimates have large standard normal deviates and hence large values of alpha, α, increasing the spread (i.e., the error variance) in the CBPCK estimate.

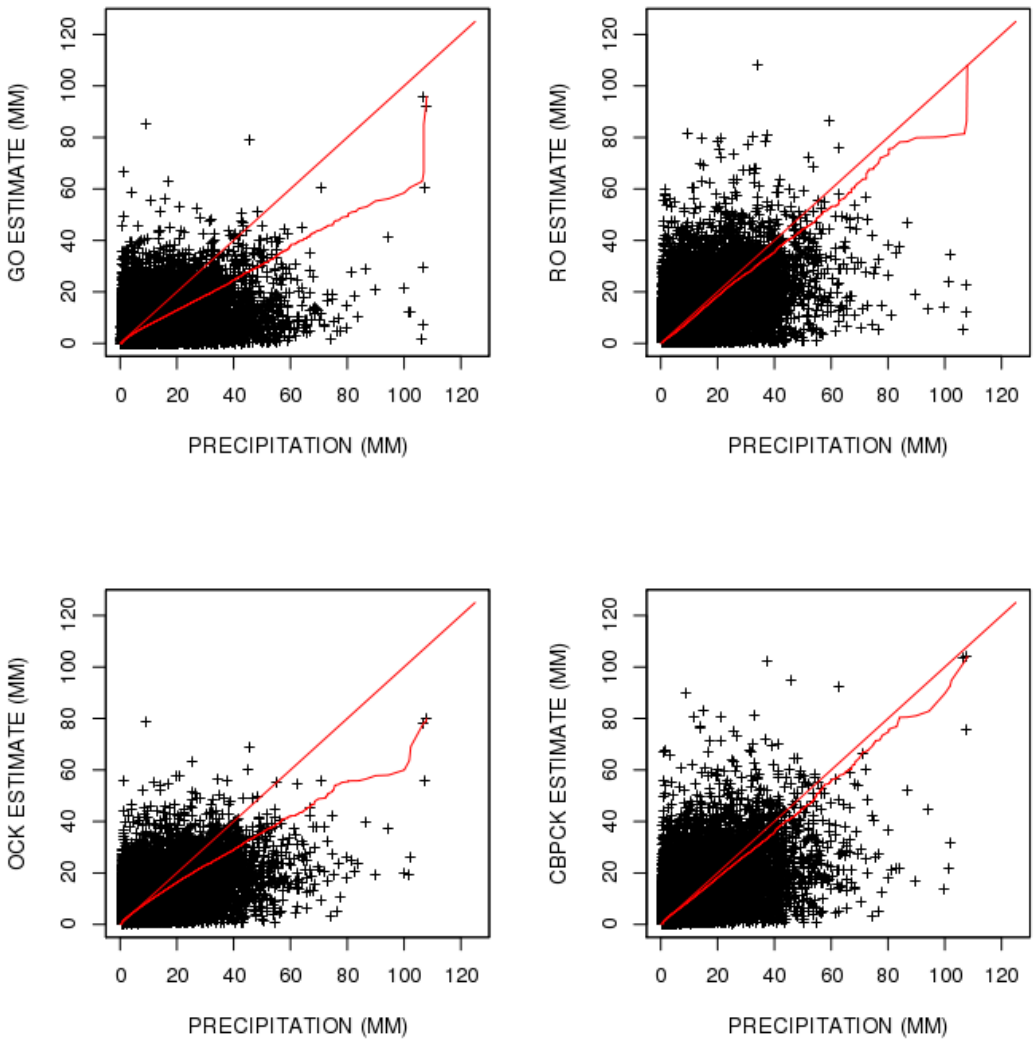

Figure 6.1 Scatter and QQ plots of the GO, RO, OCK and CBPCK estimates (2002-2008).

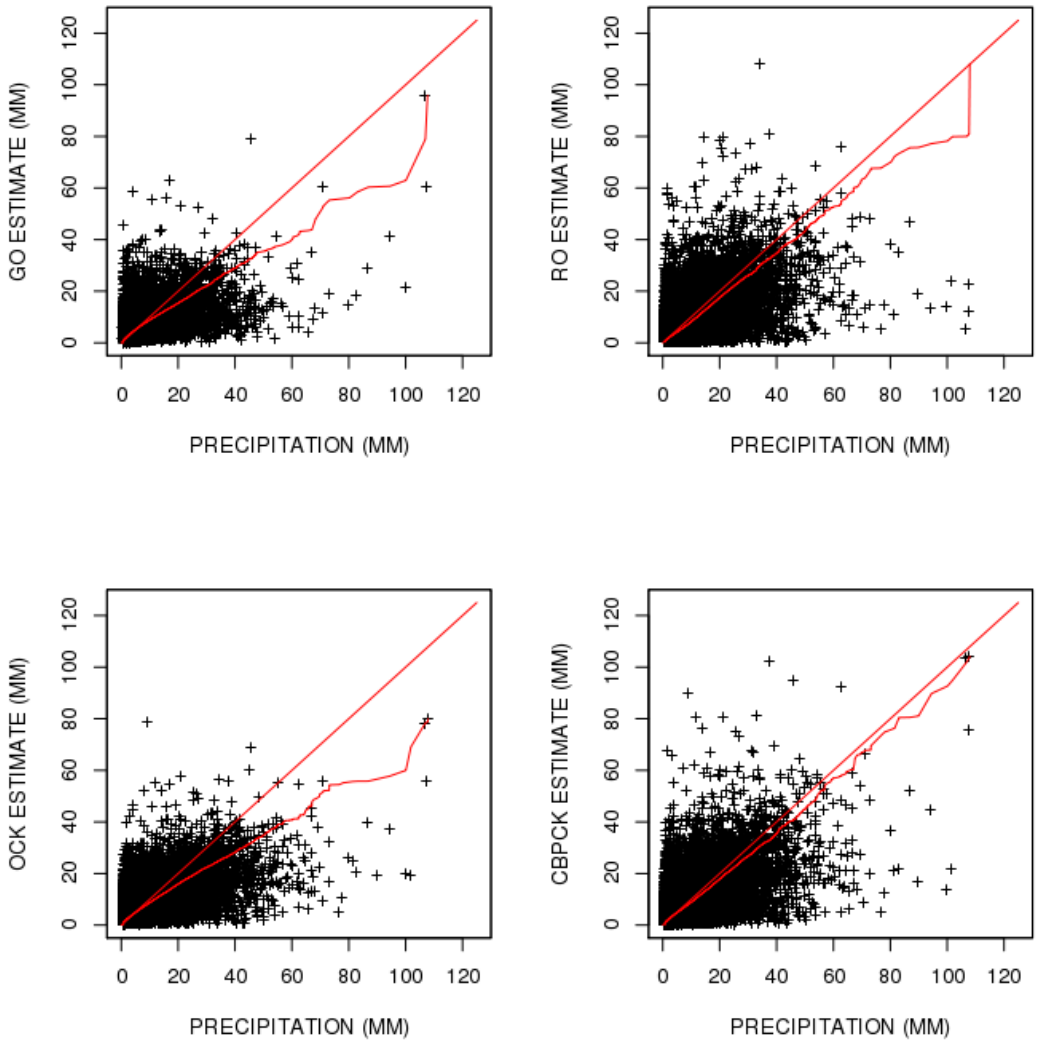

Figure 6.2 Scatter and QQ plots of the GO, RO, OCK and CBPCK estimates when FC exceeds 0.9 (2002-2008).

Figure 6.3 shows the error plot of the RO, OCK and CBPCK estimates when FC is greater than 0.9. The horizontal line of zero error means that the estimate is perfect. Note that the errors in OCK are smaller than those in RO and CBPCK for smaller precipitation amounts, and that the CBPCK estimates have significantly smaller errors for

larger amounts. Note also that the 4 data points associated with very large overestimation by CBPCK are associated with outlying OCK estimates. Eliminating occurrences of such large errors of overestimation is a challenge for which additional sources of precipitation, soft or hard, information is necessary.

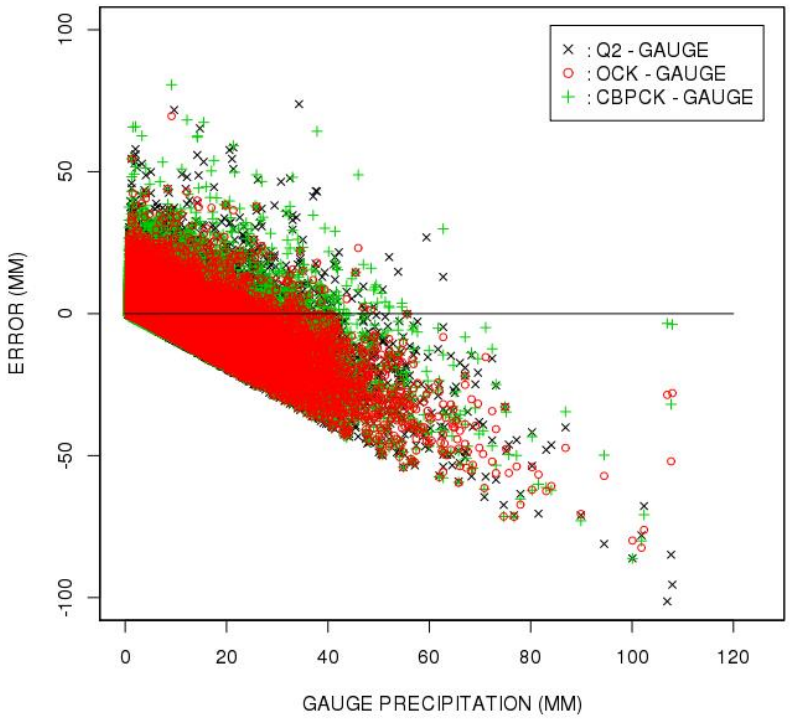

Figure 6.3 Errors in the RO, OCK and CBPCK estimates with respect to the ground truth when FC is greater than 0.9 (2002-2008).

6.1.2. Reduction in RMSE

The root mean squared error (RMSE) conditioned on the minimum threshold of gauge precipitation is used to measure the conditional performance of the estimators. The RMSE is defined as:

$$\mathrm{RMSE} = \sqrt{\frac{1}{n}\sum_{i=1}^{n}[G^*(u_i) - G(u_i)]^2} \qquad (6.1)$$

where $G^*(u_i)$ denotes the estimated precipitation at location u_i, $G(u_i)$ denotes the rain gauge precipitation at location u_i and n denotes the total number of observations. Figure 6.4 shows the reduction in RMSE by OCK over RO and by CBPCK over RO conditional on the verifying gauge precipitation greater than that shown on the x-axis. The reduction in RMSE is conditioned also on FC. For all conditions of FC, little or no reduction in RMSE is seen until the threshold precipitation begins to exceed 60 mm. For FC > 0.9, on the other hand, clear improvements are shown in both OCK and CBPCK over all ranges of the thresholding precipitation amount. Note also that the margin of improvement by CBPCK is greater than that by OCK when FC is high.

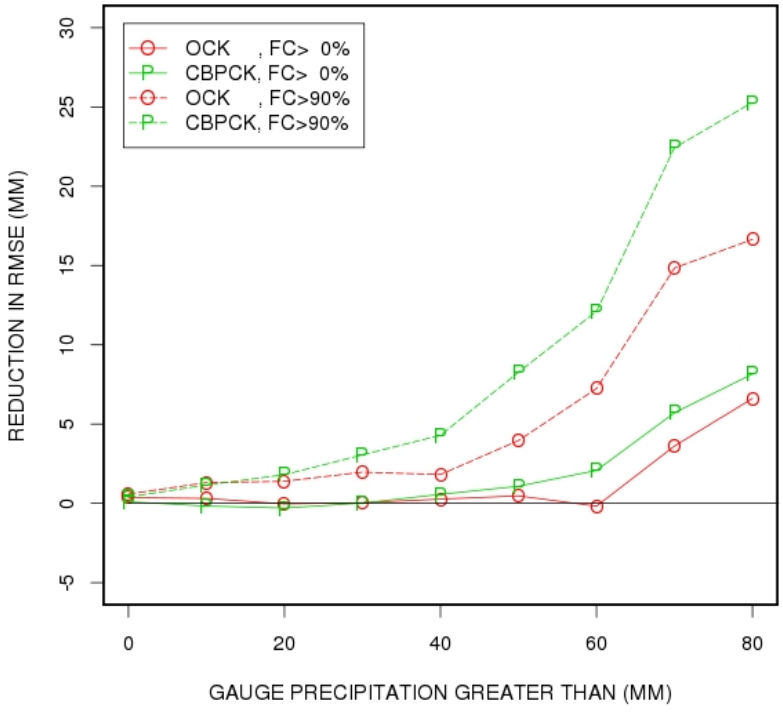

Figure 6.4 Reduction in RMSE by OCK over RO and by CBPCK over RO (2002-2008).

In addition to a reduction in RMSE, the percent reduction in RMSE (PRIRMSE) by CBPCK over OCK, or $PRiRMSE(CBPCK)$, is calculated:

$$PRiRMSE(CBPCK) = \frac{RMSE(OCK) - RMSE(CBPCK)}{RMSE(OCK)} \times 100 \quad (6.2)$$

where $RMSE(CBPCK)$ and $RMSE(OCK)$ denote the RMSEs of CBPCK and OCK estimates, respectively. Figure 6.5 shows the percent reduction in RMSE as a function of the minimum FC of precipitation over the ungauged location by CBPCK over OCK for hourly gauge precipitation intensity greater than the amount shown on the x-axis. The figure shows that CBPCK is superior to OCK for precipitation amounts greater than 30 mm regardless of FC. For FC > 0.5, the reduction is positive when gauge precipitation exceeds approximately 15 mm and, for verifying precipitation exceeding 40 mm, the reduction is about 8%. If the threshold gauge precipitation is less than 10 mm, however, CBPCK is inferior to OCK regardless of FC. The negative reduction in light precipitation arises from the fact that OCK minimizes unconditional error variance and hence does better than CBPCK for precipitation amounts around the median. Figure 6.5 also shows that, the larger the precipitation amount is, the larger the percent reduction in RMSE by CBPCK is over OCK, and that, the larger the FC is, the larger the percent reduction in RMSE is.

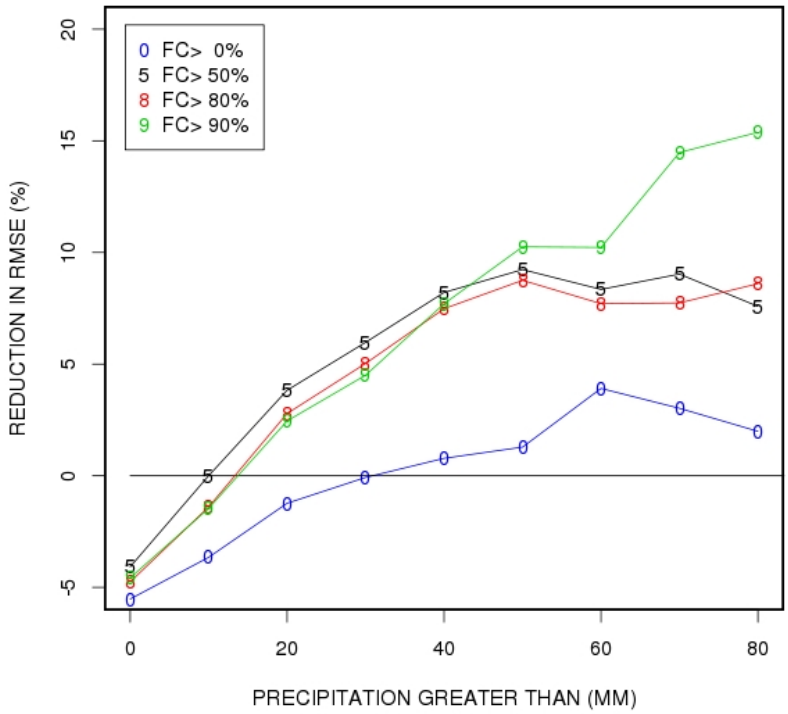

Figure 6.5 Percent reduction in RMSE as a function of the minimum FC over the ungauged location by CBPCK over OCK for hourly point precipitation amounts greater than that shown on the x-axis (2002-2008).

6.1.3. Conditional Mean

Figure 6.6 shows the conditional mean of the gauge (denoted as truth), RO, OCK and CBPCK estimates for hourly point precipitation amounts greater than that shown on the x-axis for FC > 0. Figure 6.7 is the same as Figure 6.6 but for FC > 0.9. The figure indicates that CBPCK reduces conditional mean bias over OCK for all ranges and over RO for precipitation amounts exceeding 50 mm. The margin of improvement by CBPCK over OCK increases as the threshold of verifying precipitation increases.

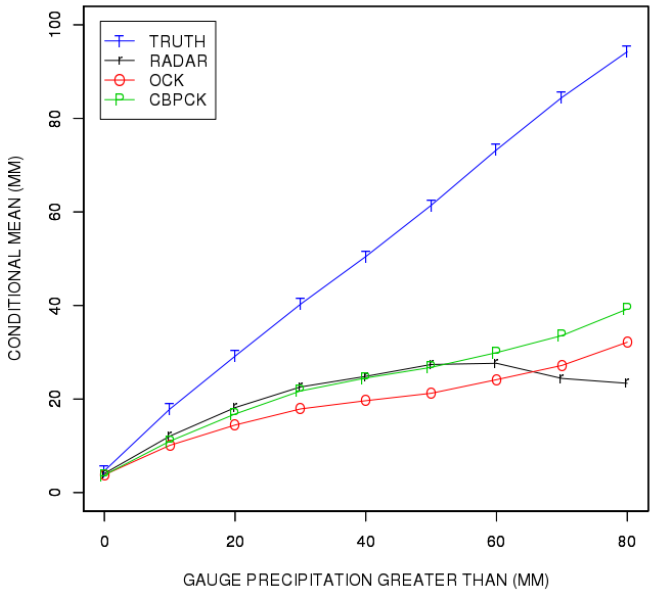

Figure 6.6 Conditional mean of the gauge (denoted as truth), RO, OCK and CBPCK estimates for FC > 0 (2002-2008).

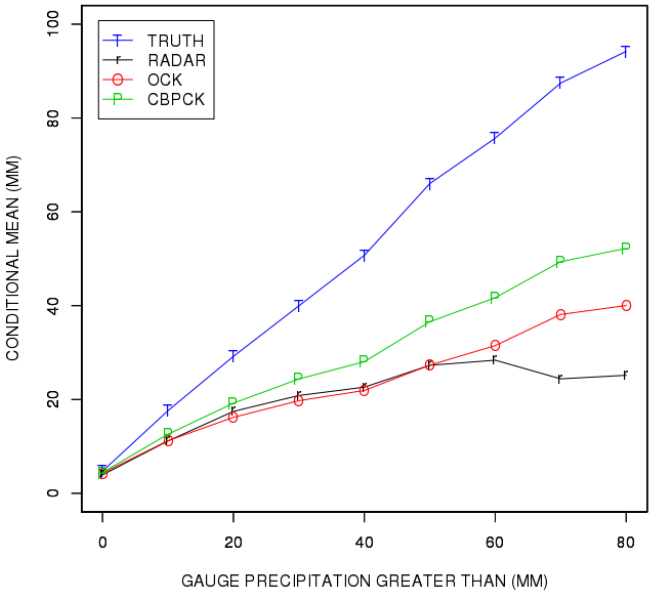

Figure 6.7 Conditional mean of the gauge (denoted as truth), RO, OCK and CBPCK estimates for FC > 0.9 (2002-2008).

6.1.4. Multiplicative Bias

The multiplicative bias is defined as the ratio of the sum of the estimates to the sum of the verifying observations:

$$\text{Multiplicative Bias} = \frac{\sum_{i=1}^{n} G^*(u_i)}{\sum_{i=1}^{n} G(u_i)} \tag{6.3}$$

Figure 6.8 shows the multiplicative bias of OCK and CBPCK estimates conditional on the verifying precipitation exceeding the threshold for FC > 0 and FC > 0.9. Large biases are observed both in the OCK and CBPCK estimates for large precipitation amounts for FC > 0. The biases are significantly reduced for FC > 0.9 in reflection of the observations above that, when FC is large, improvement by CBPCK over OCK is larger. As observed above, the margin of reduction in multiplicative bias by CBPCK over OCK also increases as the thresholding gauge precipitation increases.

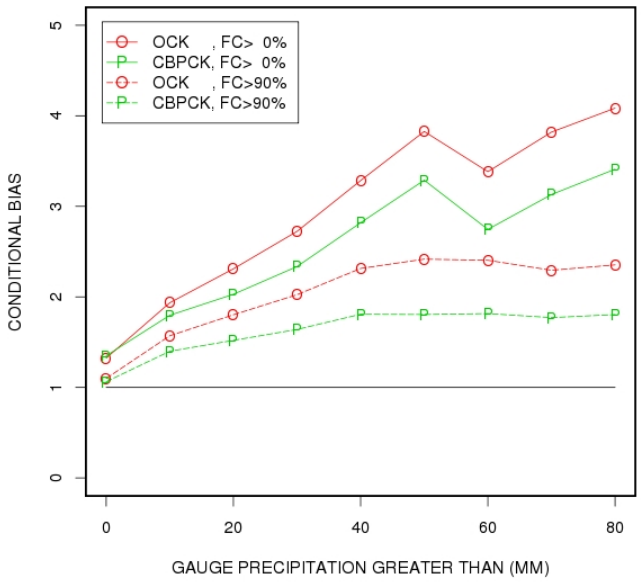

Figure 6.8 Multiplicative bias of the estimate (y-axis) conditional on verifying precipitation exceeding the threshold (x-axis) for FC > 0 (solid line) and for FC > 0.9 (dashed line) (2002-2008).

6.2. Bias Correction

In this section, the impact of bias correction in radar-only QPE is evaluated. The OCK and CBPCK techniques, as formulated in this work, assume that the radar precipitation estimates are unbiased. In reality, however, the radar QPE may be biased due to numerous error sources. If the bias is known in advance as precipitation reanalysis, one may improve the quality of multisensor QPE by combining the rain gauge observations and bias-corrected radar QPE. Bias correction is applied here by multiplying the bias correction factor to radar QPE. The bias correction factor β defined as:

$$\beta = \frac{\sum_i^n G_i(u_i)}{\sum_i^n R_i(u_i)} \tag{6.4}$$

The summations in Eq.(6.4) include only the pairs of positive gauge precipitation and positive radar precipitation.

6.2.1. Global Bias Correction

The global bias correction factor is a single number calculated using Eq.(6.4) from all available data in the entire analysis period. Here, a 4-yr analysis period of 2008 to 2011 is considered. The global bias correction factor estimated for this period is 0.90. Figure 6.9 shows the scatter plots of the GO, RO, OCK and CBPCK estimates after global bias correction. Both the scatter and QQ plots of RO vs. verifying observations show the positive impact of bias correction. The GO estimates are not influenced by the bias correction but the scatter plots of the GO are shown for comparison.

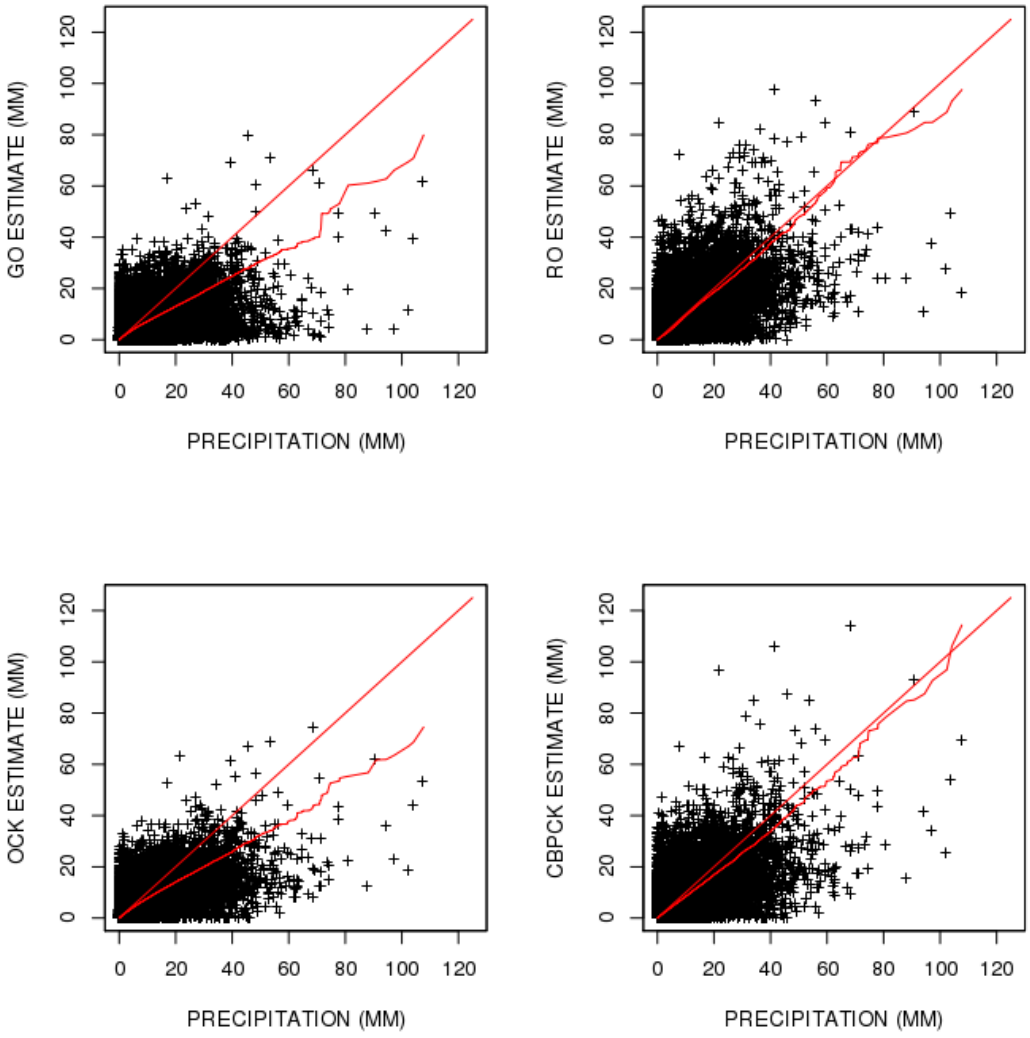

Figure 6.9 Scatter and QQ plots of the GO, RO, OCK and CBPCK estimates after global bias correction (2008-2011).

The scatter plots of hourly estimates are often difficult to compare visually due to large variability. Figure 6.10 shows the scater and QQ plots of the monthly GO, RO, OCK and CBPCK estimates following global bias correction of radar QPE. The value of multisensor estimation is readily seen. As noted above, CB is an issue largely at subdaily

time scales. As such, one may expect CBPCK to approach OCK as the time scale of aggregation increases. It is interesting to note that, albeit small, the positive impact of CBPCK relative to OCK is seen in reducing CB even at monthly scale.

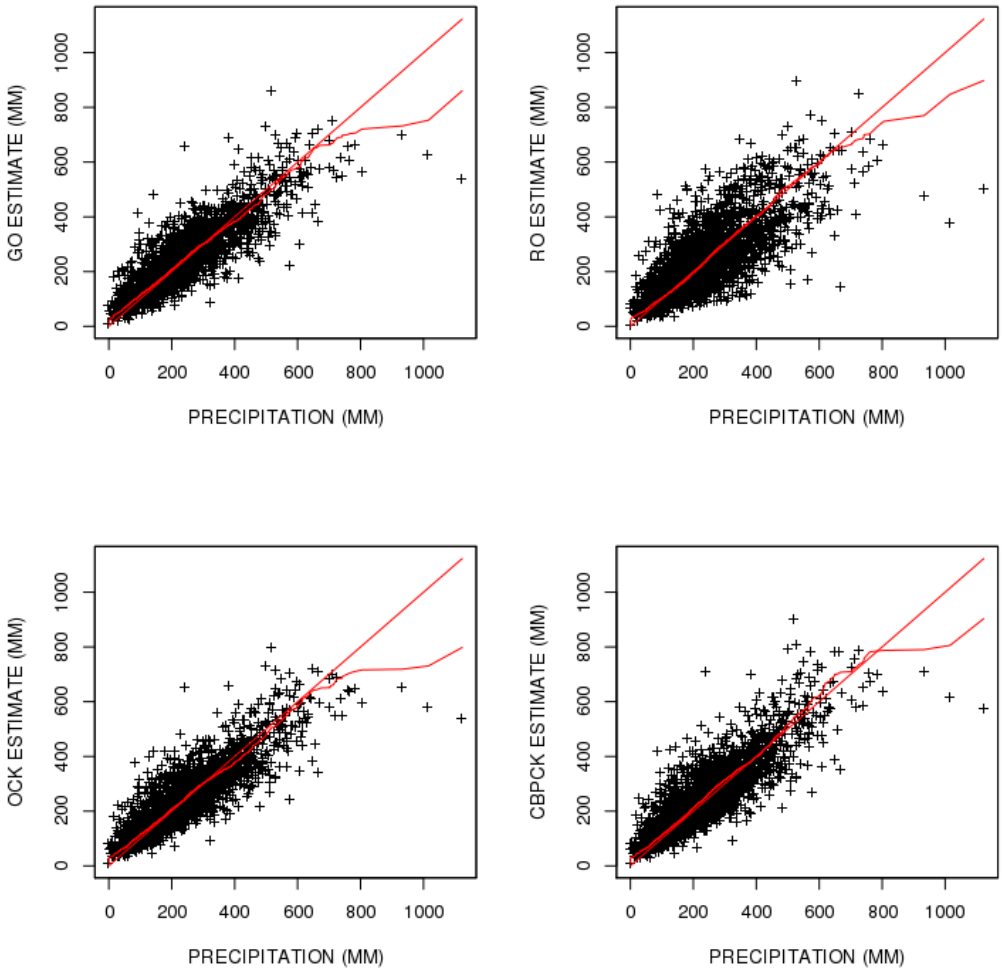

Figure 6.10 Scatter and QQ plots of the monthly GO, RO, OCK and CBPCK estimates after global bias correction (2008-2011).

6.2.2. Monthly Bias Correction

In this approach, the bias correction factor is calculated for every month for the same 4-yr period to consider the seasonal bias. Figure 6.11 shows the monthly bias correction factors averaged over 4 years. The results indicate that the radar QPE generally over- and underestimate the gauge precipitation during the warm and cool seasons, respectively.

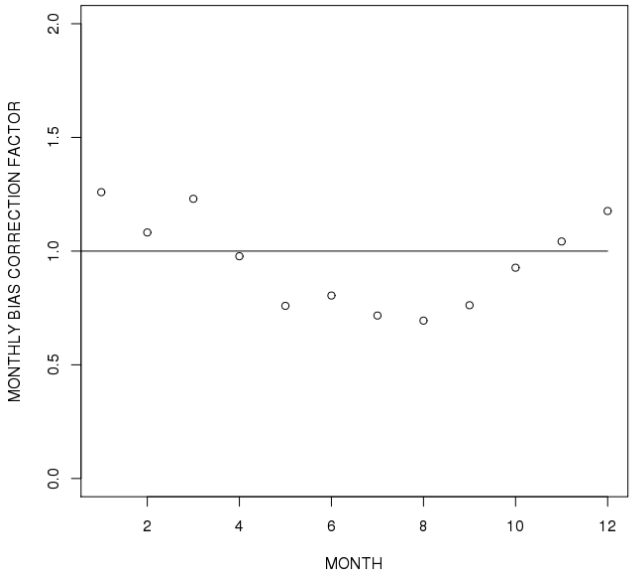

Figure 6.11 Monthly bias correction factor for radar QPE (2008-2011).

Figure 6.12 shows the scatter and QQ plots of the GO, monthly bias-corrected RO, OCK and CBPCK estimates after monthly bias correction to radar data. Compared to the global bias correction results, the generally reduced scatter in all estimates may be seen. It may also be seen that the CBPCK estimates have the smallest CB for larger precipitation amounts. Figure 6.13 shows the scatter and QQ plots of the monthly GO, RO, OCK and CBPCK estimates after monthly bias correction. Note that both OCK and CBPCK are clearly closer to the true precipitation compared to RO.

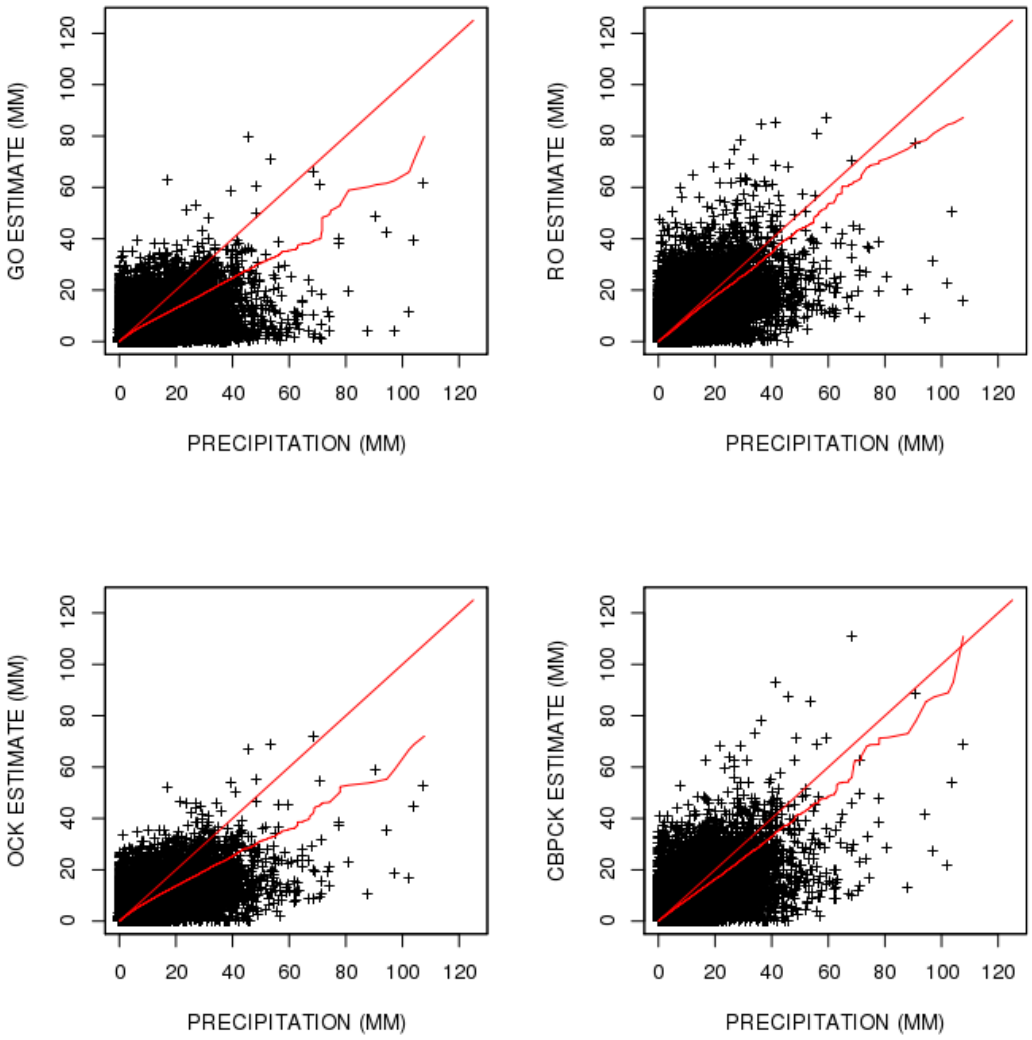

Figure 6.12 Scatter and QQ plots of the GO, RO, OCK and CBPCK estimates after monthly bias correction (2008-2011).

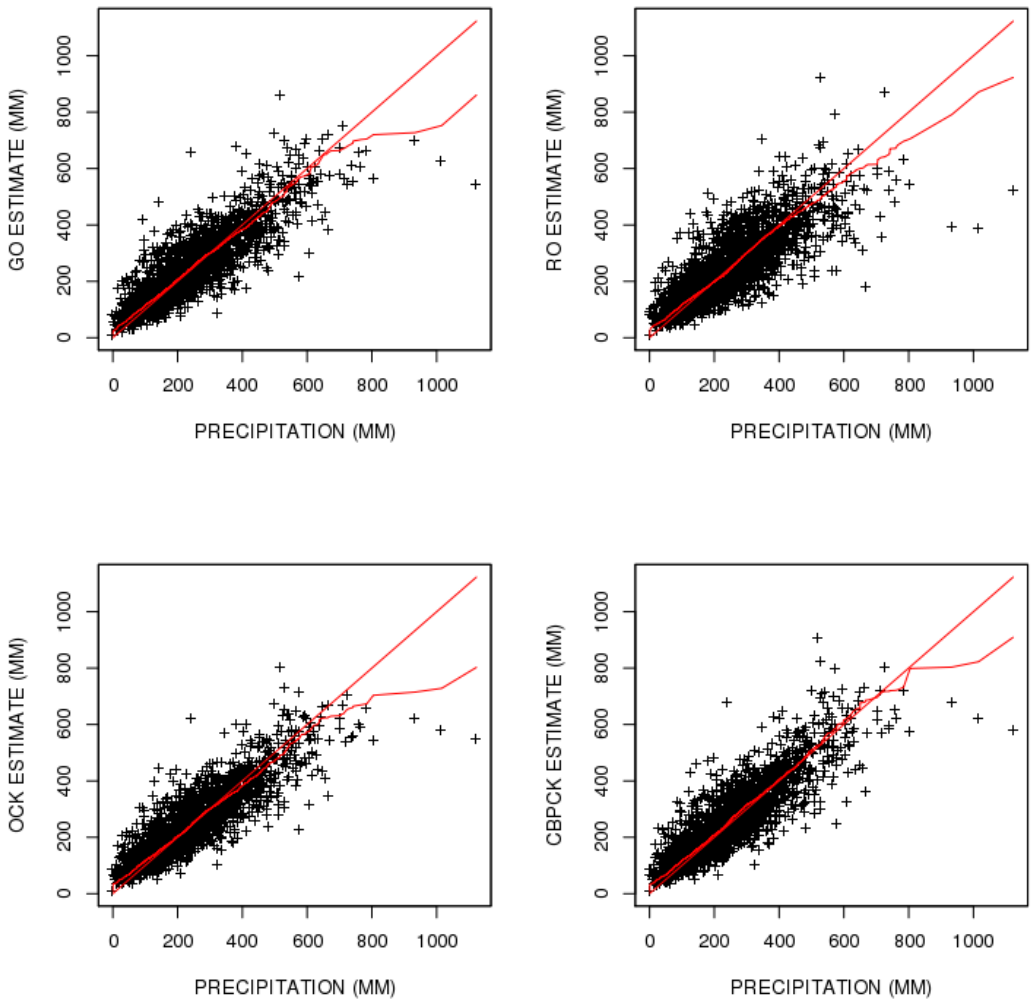

Figure 6.13 Scatter and QQ plots of the monthly GO, RO, OCK and CBPCK estimates after monthly bias correction (2008-2011).

Figure 6.14 shows the percent reduction in RMSE by OCK over RO and by CBPCK over RO after monthly and global bias correction. OCK is inferior to RO over thresholds less than 50 mm. CBPCK, on the other hand, is superior or comparable to RO at all thresholds. For large precipitation amounts, significant reduction of up to 20% in RMSE by CBPCK over RO is seen. Compared to global bias correction, the relative

performance by OCK over RO after monthly bias correction is slightly improved. The relative performance by CBPCK over RO, on the other hand, does not changed much with the different bias correction methods.

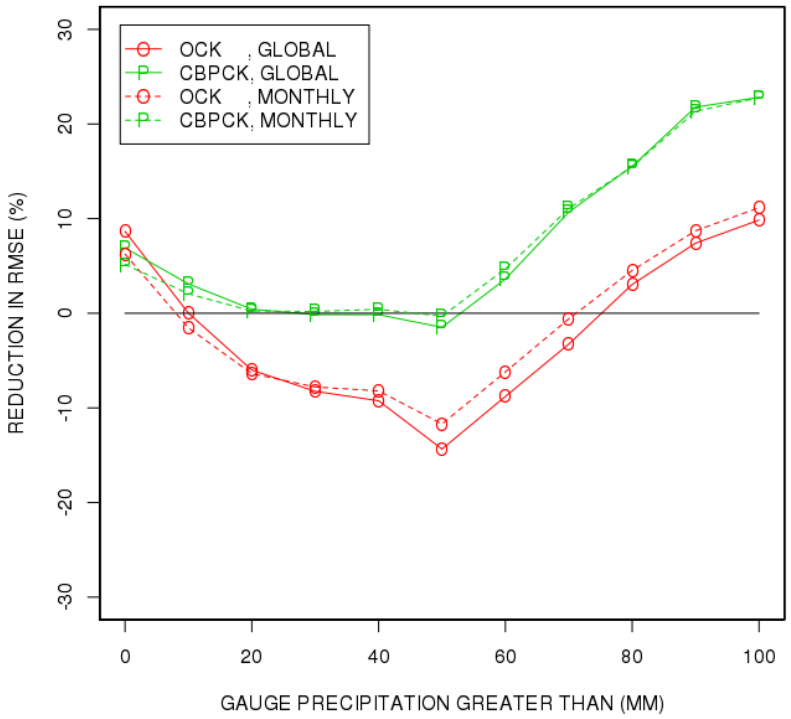

Figure 6.14 Percent reduction in RMSE by OCK over RO and by CBPCK over RO after bias correction (2008-2011).

6.3. Monthly Events Analysis

While the global analysis over long analysis periods is useful for assessment of long-term performance, the relative performance among GO, RO, OCK and CBPCK may depend greatly on specific rainfall events that produce very large to extreme amounts of precipitation. Event-specific evaluation of the techniques, however, was beyond the scope of this work. As a compromise, the scatter plots of hourly estimates were visually examined for a number of specific months that produced large amounts of precipitation. Figure 6.15 through 6.21 show the scatter and QQ plots of the hourly estimates of GO, RO, OCK and CBPCK vs. the verifying precipitation for the month shown in each figure. The generally positive impact of multisensor estimation and specifically of CBPCK, may be seen. The figures also illustrate the limitation of CBPCK. In this subsection, monthly bias corrected radar QPE is used (denotes as RO for brevity).

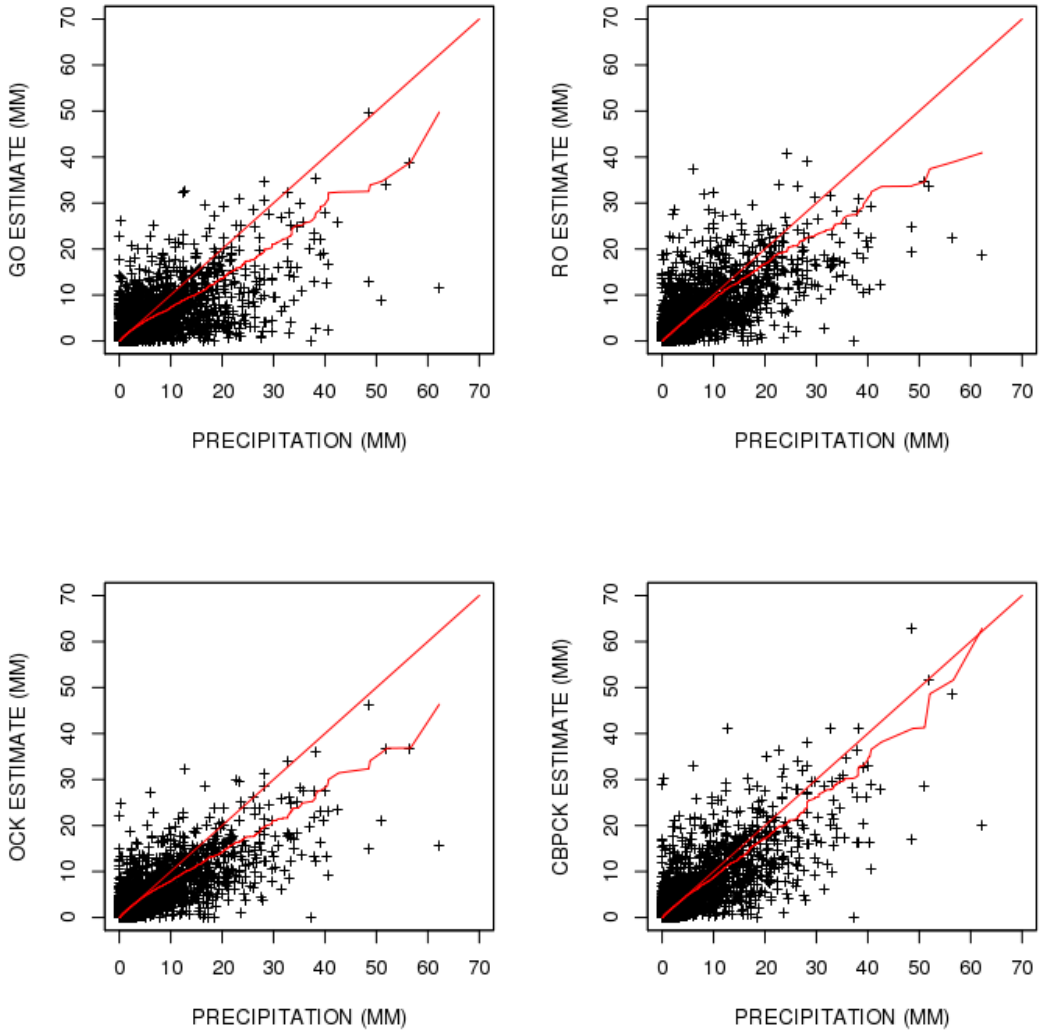

Figure 6.15 Scatter and QQ plots of the hourly estimates (April, 2008)

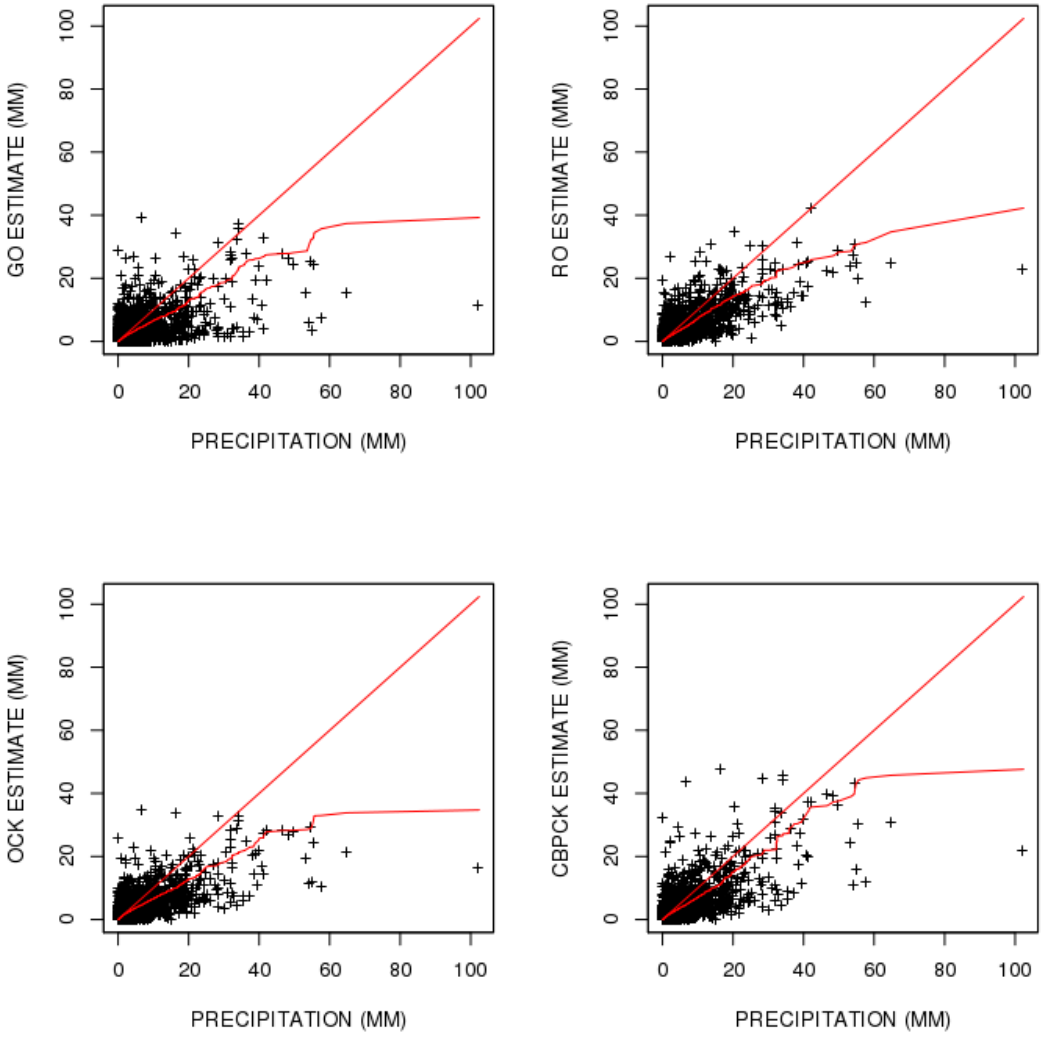

Figure 6.16 Scatter and QQ plots of the hourly estimates (June, 2008)

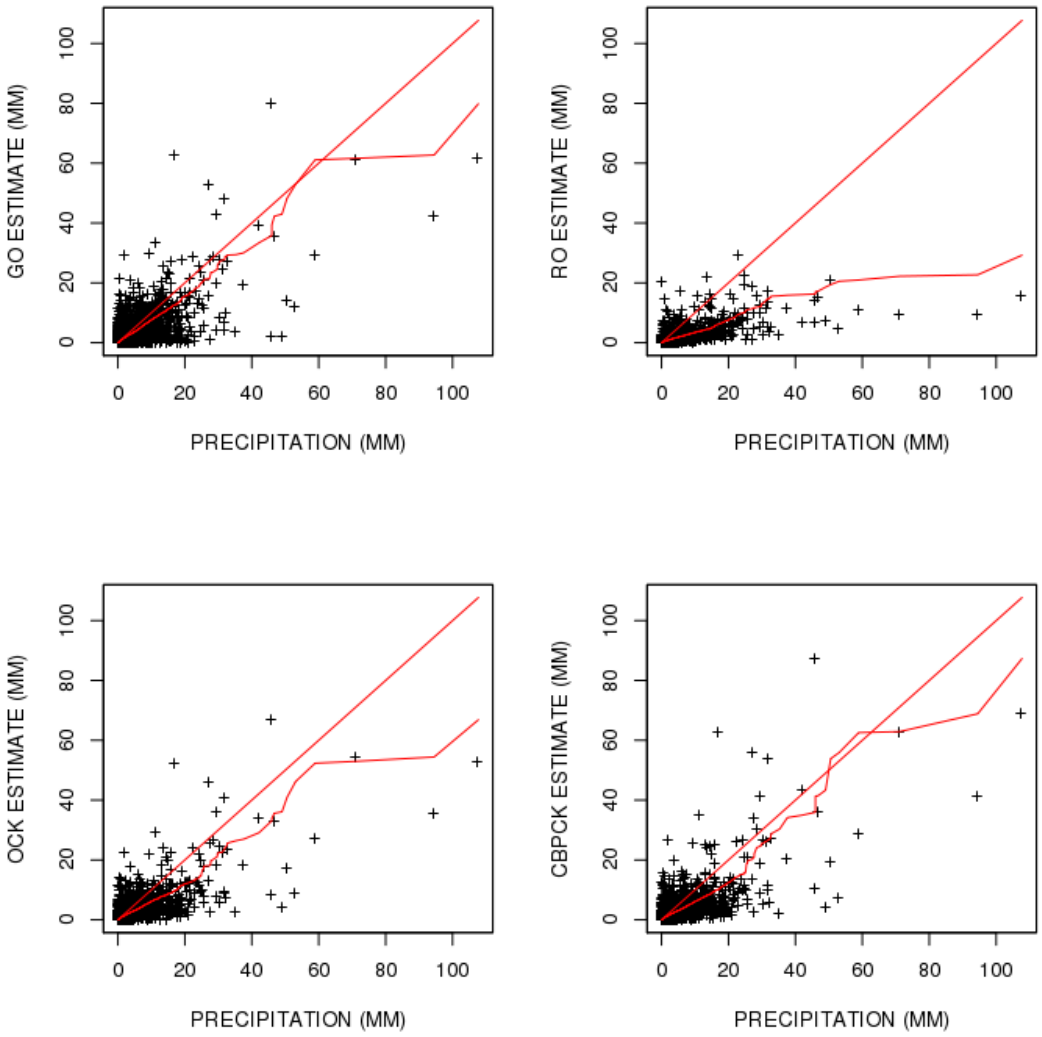

Figure 6.17 Scatter and QQ plots of the hourly estimates (September, 2008)

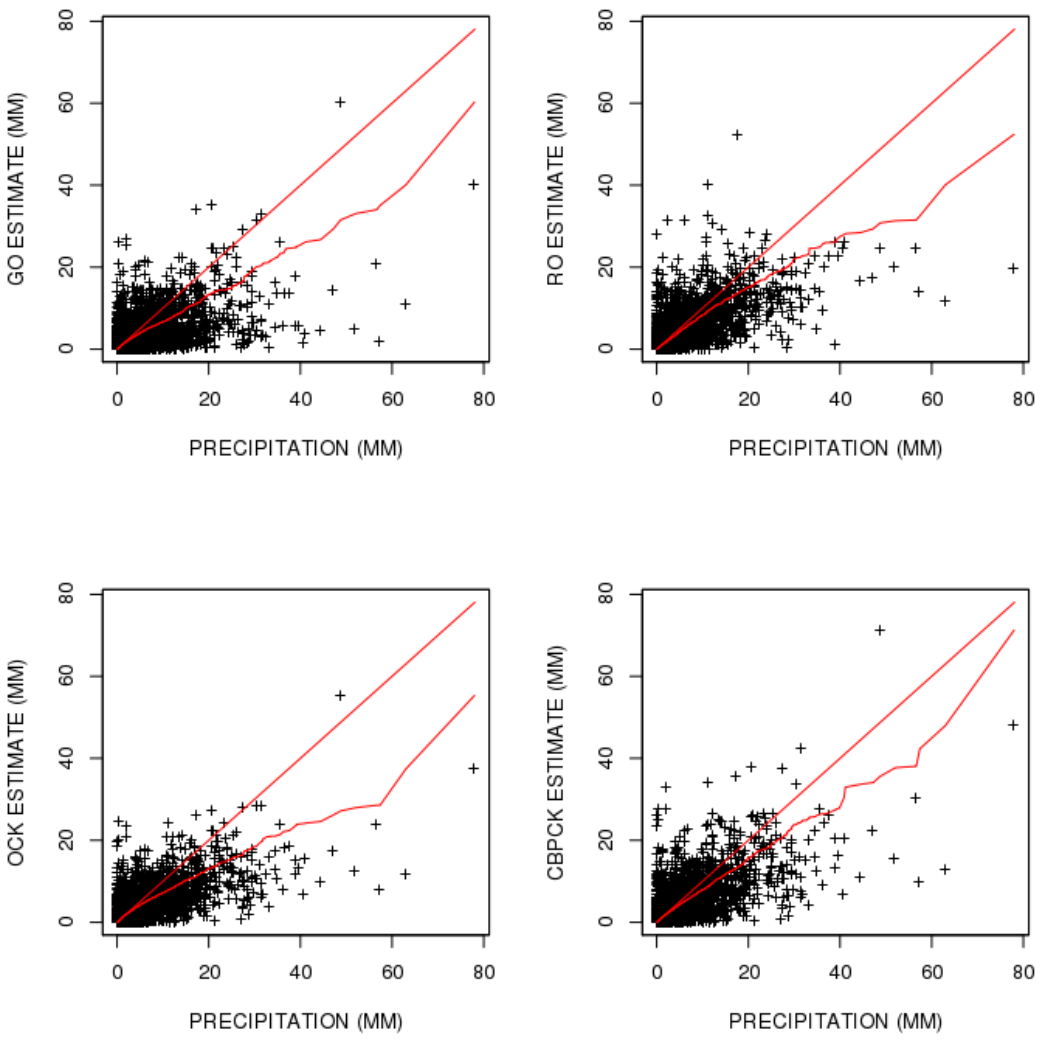

Figure 6.18 Scatter and QQ plots of the hourly estimates (May, 2009)

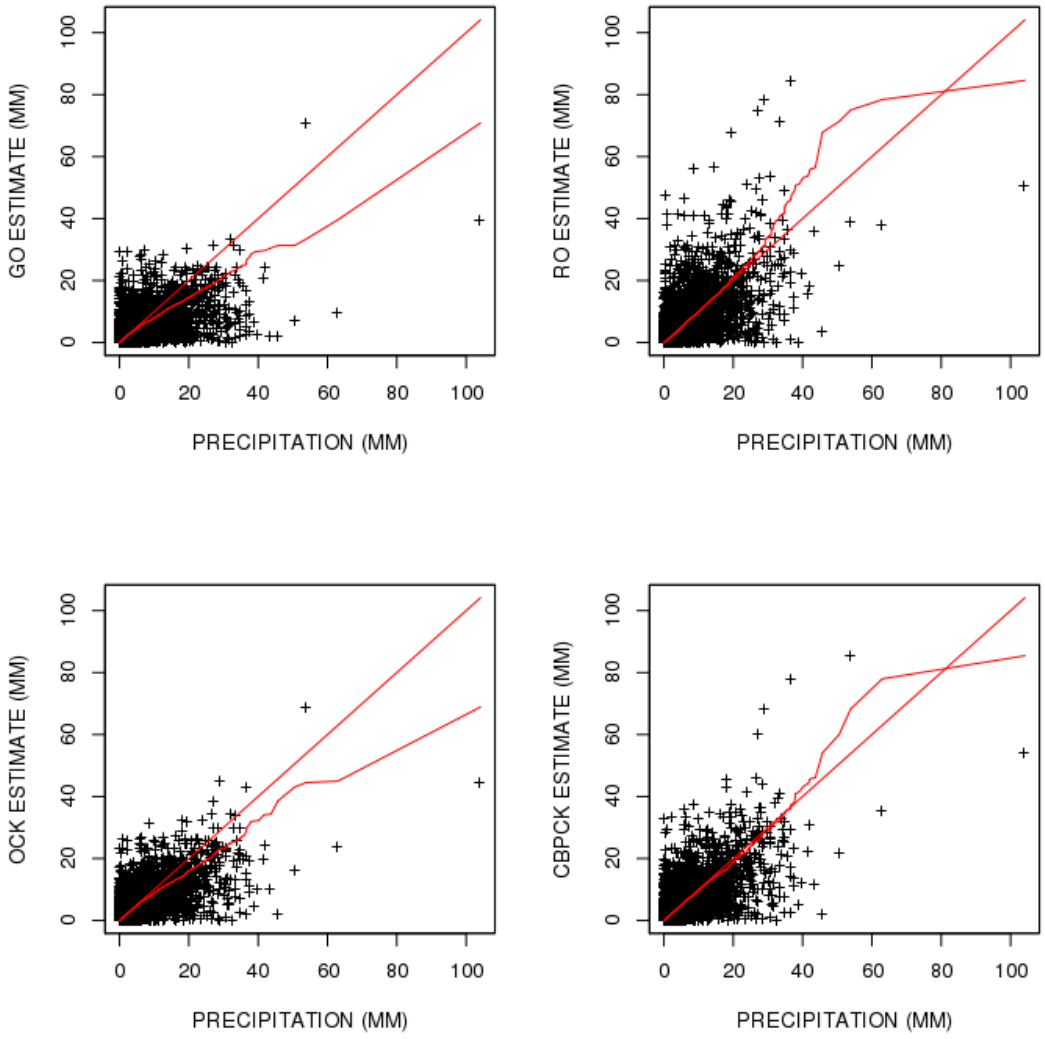

Figure 6.19 Scatter and QQ plots of the hourly estimates (October, 2009)

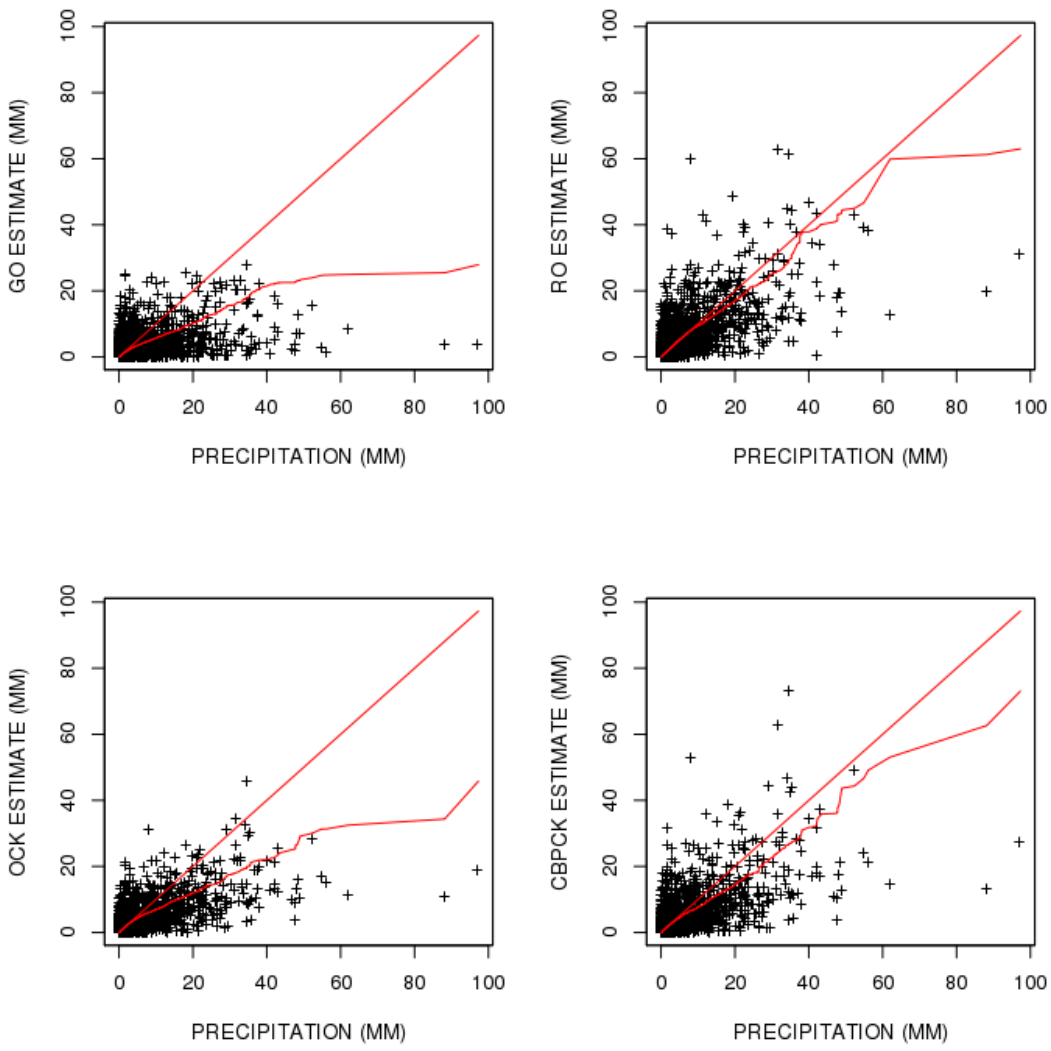

Figure 6.20 Scatter and QQ plots of the hourly estimates (June, 2010)

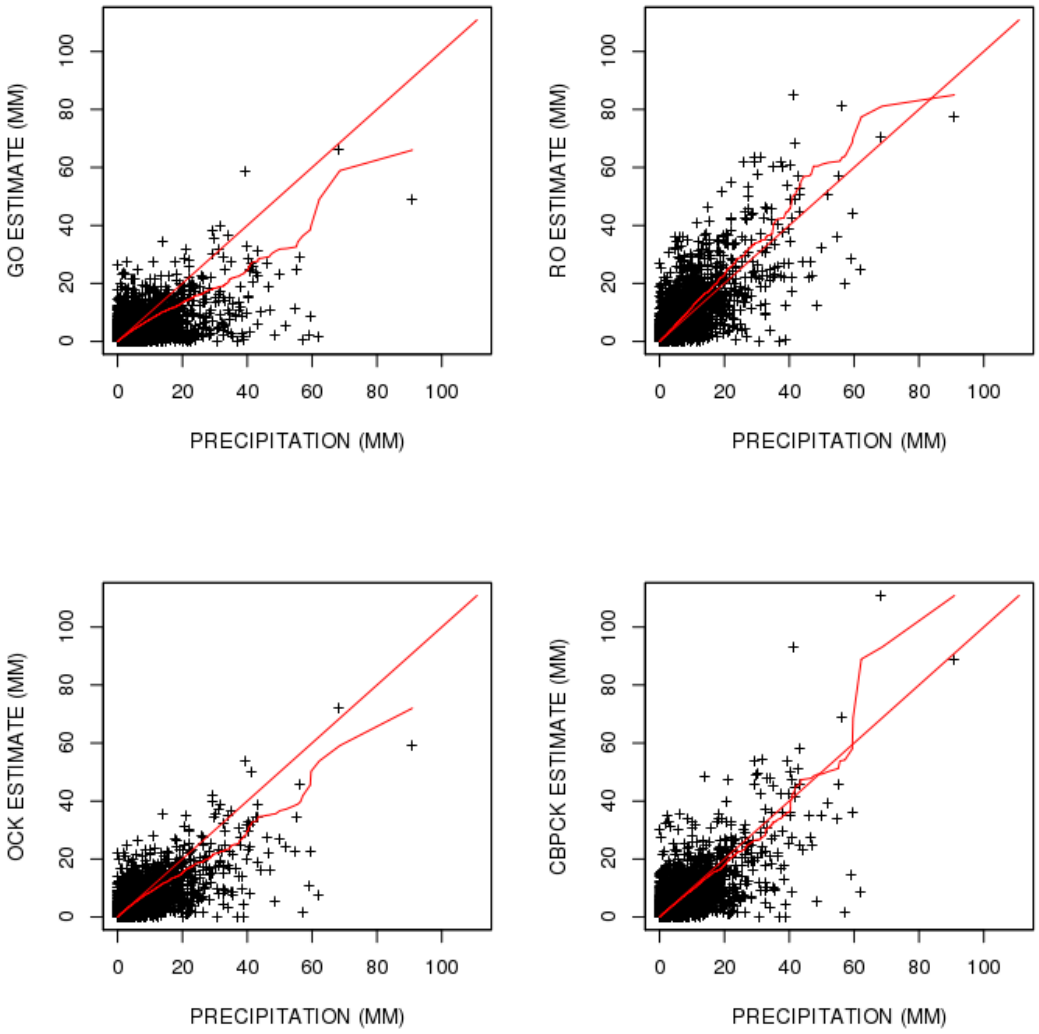

Figure 6.21 Scatter and QQ plots of the hourly estimates (September, 2010)

6.4. Visual Examination of Merged Fields

In this subsection, the hourly multisensor analyses are accumulated up to a month for visual assessment of the performance of each technique. Unlike cross validation, all data points within the analysis domain of GO, RO, OCK and CBPCK estimates are included in the scatter plot and the QQ plot. In this subsection, monthly bias corrected radar QPE is used (denotes as RO for brevity).

6.4.1. Hourly Analysis

Figure 6.22 shows an example of the hourly field of GO, RO, OCK and CBPCK analyses. The GO field is generated using ECBPK (Seo et al., 2014).The complementary nature of the multisensor analyses is readily seen. Note also that, compared to the OCK analysis, the CBPCK analysis shows increased precipitation in the convective cores, and that, to improve analysis, it is necessary to model anisotropy.

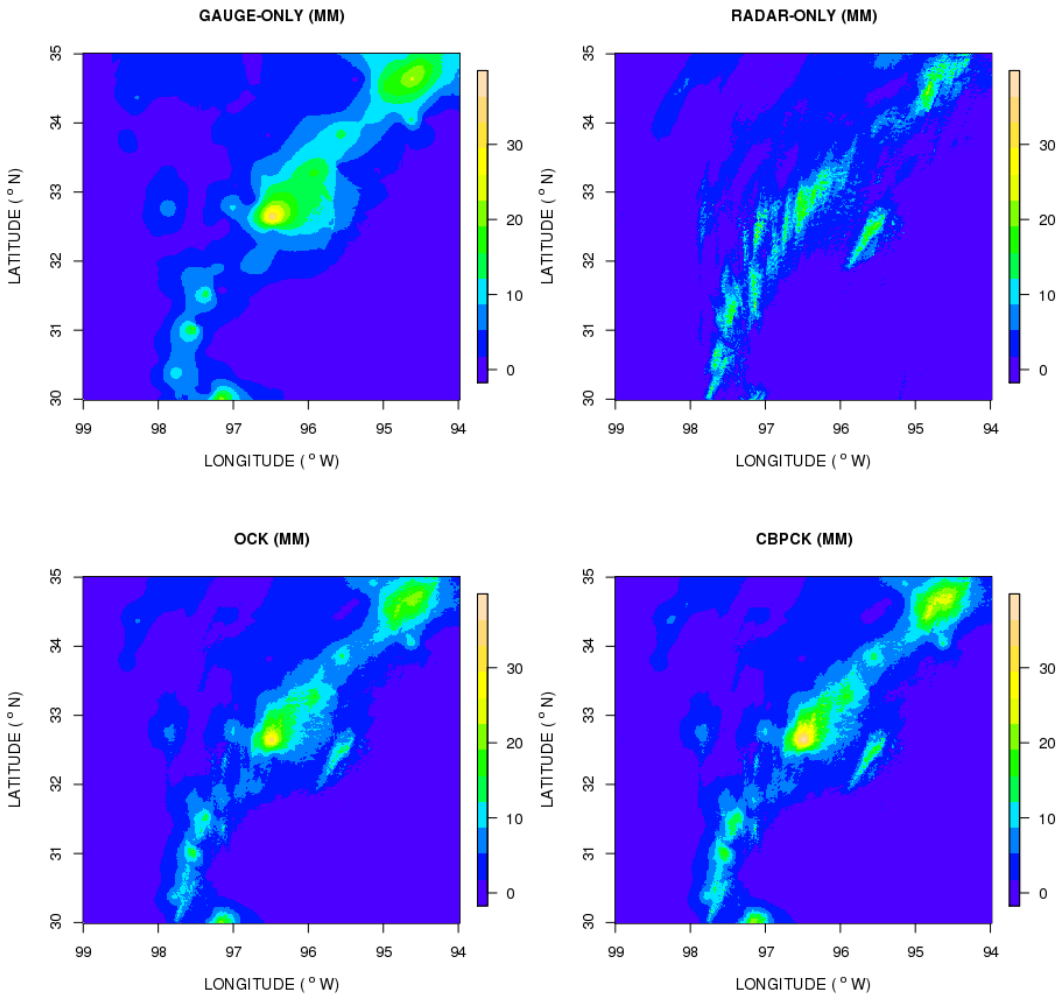

Figure 6.22 Examples of hourly precipitation analysis by GO (upper-left), RO (upper-right), OCK (lower-left) and CBPCK (lower-right) valid at 9 pm on March 18, 2008.

6.4.2. Daily Analysis

Figure 6.23 shows the examples of daily precipitation based on hourly GO (upper-left), RO (upper-right), OCK (lower-left) and CBPCK (lower-right) on March 18, 2008. Note that, the daily fields are generated by accumulating the hourly analyses as opposed to by analysis using daily precipitation data. Similar observations to the hourly example above may be made. Figure 6.24 shows the scatter and QQ plots of daily precipitation for RO vs. GO (upper-left), OCK vs. GO (upper-right), CBPCK vs. GO (lower-left) and CBPCK vs. RO (lower-right) analysis for March 18, 2008. It may be seen that the RO severely underestimate GO in areas of heavy precipitation. By contrast, the OCK estimates are generally in line with the GO estimates albeit somewhat lower overall precipitation amounts. CBPCK is seen to be somewhat lower than GO but slightly higher than GO for large precipitation amounts.

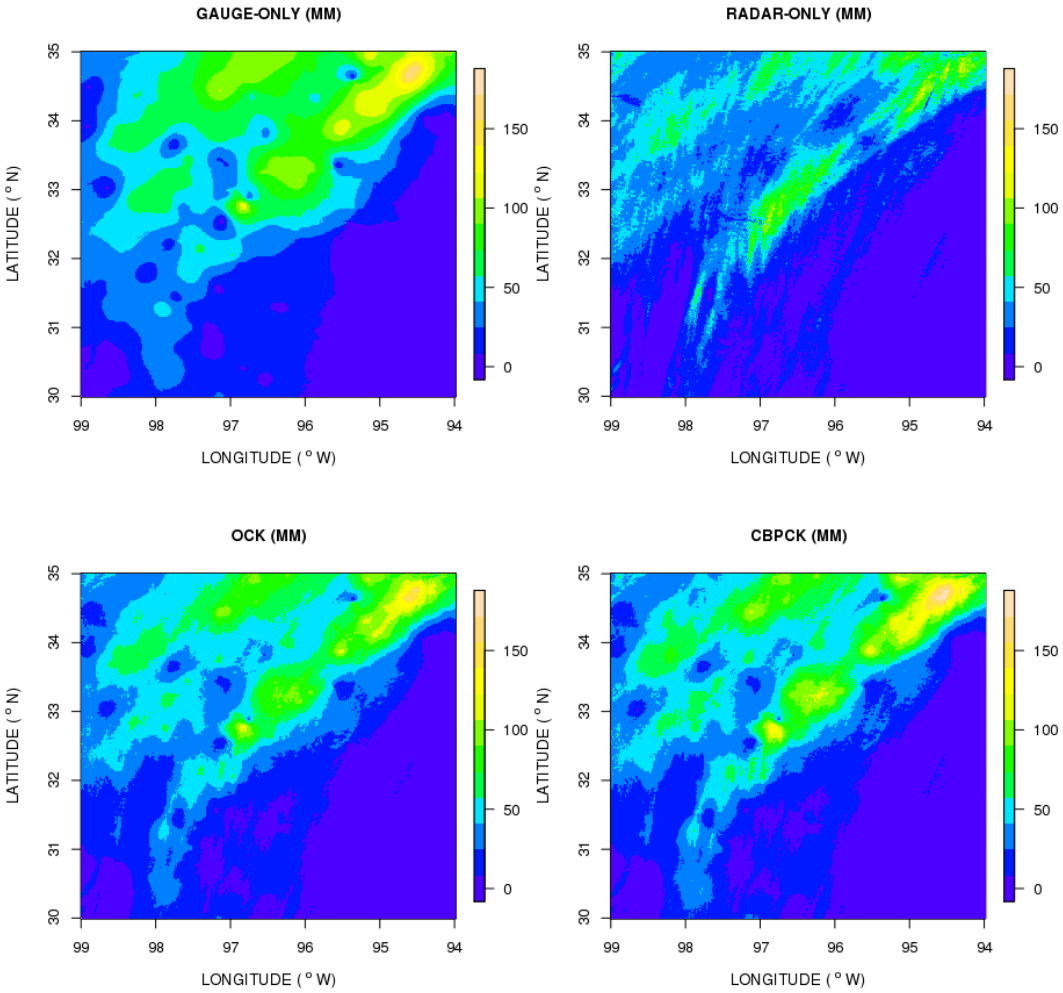

Figure 6.23 Example fields of daily precipitation by GO (upper-left), RO (upper-right), OCK (lower-left) and CBPCK (lower-right) for 18 March 18, 2008.

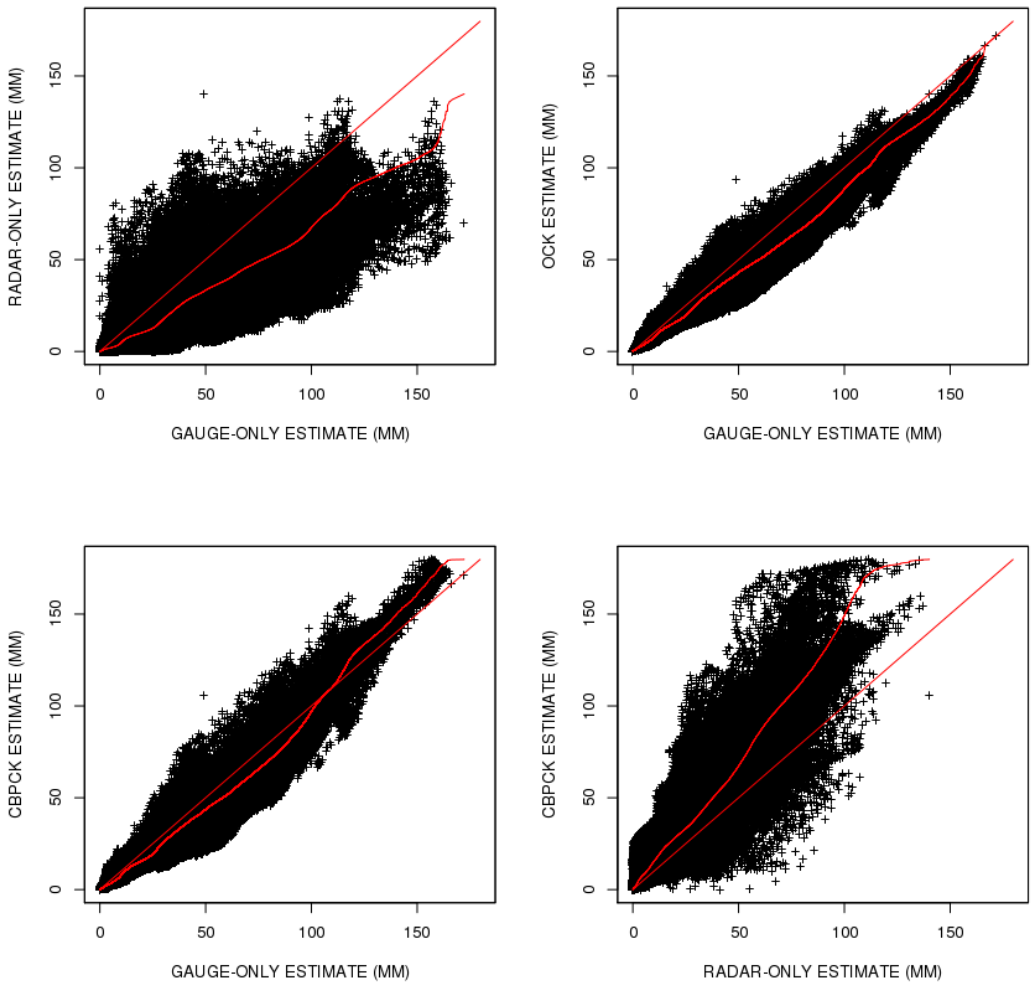

Figure 6.24 Scatter and QQ plots of daily precipitation for RO vs. GO (upper-left), OCK vs. GO (upper-right), CBPCK vs. GO (lower-left) and CBPCK vs. RO (lower-right) analysis for March 18, 2008.

6.4.3. Monthly Analysis

Figure 6.25 shows the example fields of monthly precipitation from GO (upper-left), RO (upper-right), OCK (lower-left) and CBPCK (lower-right) for March, 2008. The figure strengthens the observations made above. It is interesting to note that CBPCK shows a more RO-like precipitation patterns than OCK. While it is not possible to verify due to lack of ground truth, the above suggests that CBPCK may be better able to capture the variability.

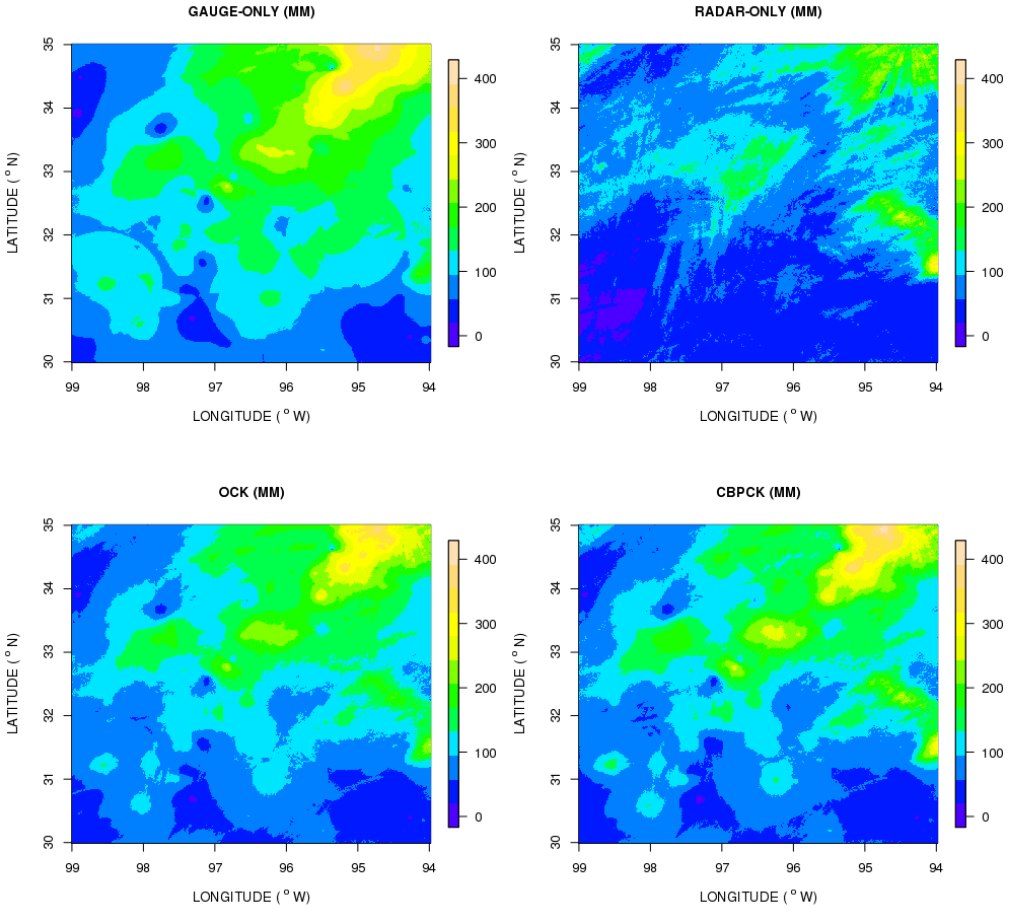

Figure 6.25 Example fields of monthly precipitation from GO (upper-left), RO (upper-right), OCK (lower-left) and CBPCK (lower-right) for March, 2008.

Figure 6.26 shows the scatter and QQ plots of monthly precipitation for RO vs. GO (upper-left), OCK vs. GO (upper-right), CBPCK vs. GO (lower-left) and CBPCK vs. RO (lower-right) analysis for March, 2008. Compared to the OCK estimates, the CBPCK is more closely in line with the GO estimates for large precipitation amounts but shows larger variability.

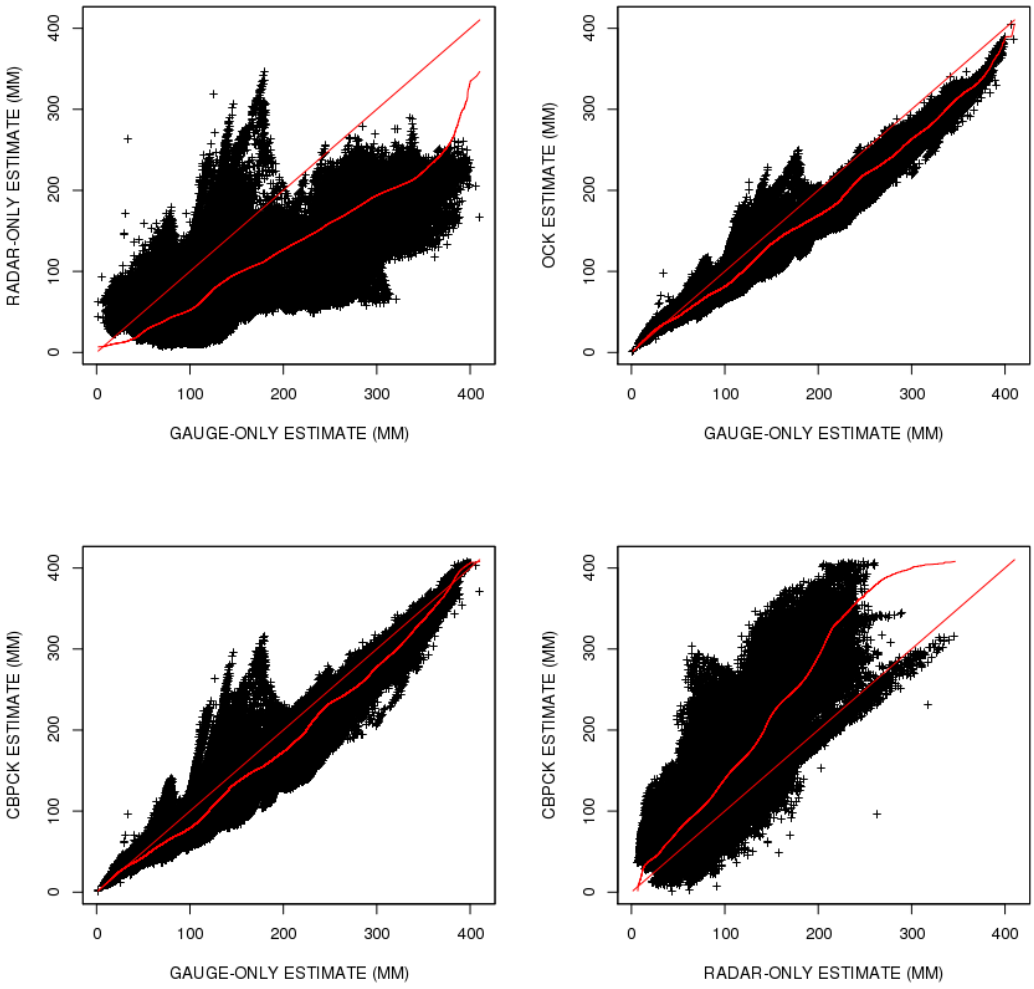

Figure 6.26 Scatter and QQ plots of monthly precipitation for RO vs. GO (upper-left), OCK vs. GO (upper-right), CBPCK vs. GO (lower-left) and CBPCK vs. RO (lower-right) analysis for March, 2008.

Finally, Figure 6.27 shows the difference between the monthly OCK and CBPCK estimates for March, 2008. The difference ranges from negative 25 mm to positive 70 mm. It may be seen that CBPCK significantly increases estimates in areas of heavy precipitation while decreasing over areas of light precipitation.

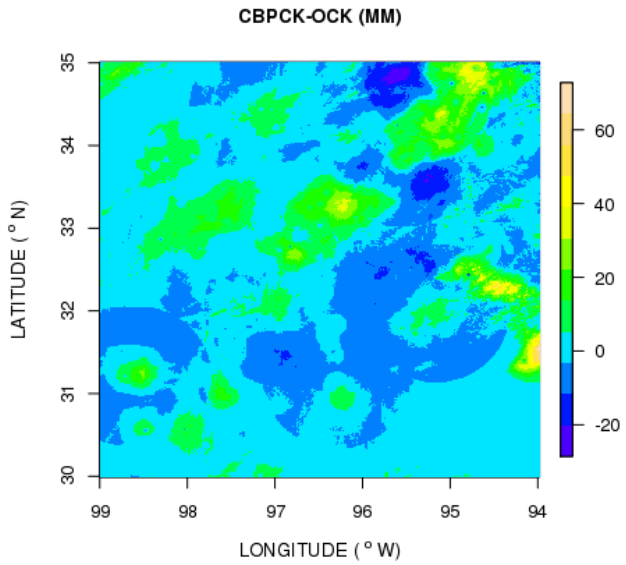

Figure 6.27 Difference between the monthly OCK and CBPCK estimates for March, 2008.

Chapter 7

Conclusions and Future Research Recommendations

A new multisensor QPE technique, conditional bias-penalized cokriging (CBPCK), has been developed to improve estimation of heavy-to-extreme precipitation using radar quantitative precipitation estimates (QPE) and rain gauge observations. Based on extended CBPK (ECBPK, Seo et al., 2014) developed for gauge-only analysis, CBPCK explicitly reduces Type-II conditional bias (CB) in addition to error variance. For evaluation, multi-year cross validation is carried out for CBPCK, Single Optimal Estimation (SOE, Seo, 1998 a,b) which is currently used in the NWS's Multisensor Precipitation Estimator (MPE), radar-only QPE from Q2 reanalysis (Nelson et al., 2010) and gauge-only analysis using ECBPK. SOE is a variant of ordinary cokriging (OCK) and is referred to here as OCK. The analysis domain is about 560 x 560 km^2 in the North Central Texas region. The analysis grid has a resolution of 0.01° (latitude) × 0.01° (longitude). The analysis period is from 2002 to 2011. The hourly rain gauge data used is from the Hydrometeorological Automated Data System (HADS, Kim et al., 2009). There are 199 rain gauges in the analysis domain. To quality-control the rain gauge data, a series of gauge-only and radar-gauge checks are carried out. The main findings and conclusions are as follows**.** CBPCK improves over OCK for estimation of hourly precipitation exceeding 30 mm. The margin of improvement depends most significantly on the fractional coverage (FC) of precipitation at the ungauged location. If FC is 50% or higher, CBPK reduces root mean square error (RMSE) over OCK by approximately 8%for hourly precipitation greater than 40 mm. If FC is 90% or higher (i.e., it is precipitating with near certainty), the margin of improvement is approximately 15% for hourly precipitation greater than 70 mm.

Bias correction to radar data improves the performance of both OCK and CBPCK. Compared to global bias correction, monthly bias correction is marginally more effective. The Q2 reanalysis product is found to be biased high globally by about 10%, and over and underestimates in the warm and cool seasons, respectively. The above findings suggest that monthly bias correction may suffice in multisensor precipitation reanalysis using the Q2 products (Nelson et al. 2010). Quality control of rain gauge observations remains a large challenge. For objective evaluation, there exists a clear need for high quality hourly rain gauge data. Visual examination of the analysis results at hourly, daily and monthly scales of accumulation indicates that, compared to OCK, CBPCK increases and decreases the amounts in areas of heavy and light precipitation, respectively, and that the CBPCK estimates tend to be more in line with the gauge-only estimates than the OCK estimates. There are indications, however, that the CBPCK estimates might be too high. Because the quality of the weighting factor, α, is only as good as that of the OCK estimates, there are occasions when CBPCK severely overestimates light precipitation due to mis-prognostication of the magnitude of precipitation at the ungauged location. For more skillful determination of α, it is necessary to incorporate additional sources of precipitation information, such as satellite QPE, lightning observations and numerical weather prediction (NWP) output. It points out that, to address different types of errors, it is necessary to utilize all available precipitation information.

References

Austin, P.M., 1987. Relation between Measured Radar Reflectivity and Surface Rainfall. Mon. Weather Rev. 115, 1053–1070. doi:10.1175/1520-0493(1987)115<1053:RBMRRA>2.0.CO;2

Azimi-Zonooz, A., Krajewski, W.F., Bowles, D.S., Seo, D.J., 1989. Spatial rainfall estimation by linear and non-linear co-kriging of radar-rainfall and raingage data. Stoch. Hydrol. Hydraul. 3, 51–67. doi:10.1007/BF01543427

Brown, J.D., Seo, D.-J., 2013. Evaluation of a nonparametric post-processor for bias correction and uncertainty estimation of hydrologic predictions. Hydrol. Process. 27, 83–105. doi:10.1002/hyp.9263

Ciach, G.J., Morrissey, M.L., Krajewski, W.F., 2000. Conditional Bias in Radar Rainfall Estimation. J. Appl. Meteorol. 39, 1941–1946. doi:10.1175/1520-0450(2000)039<1941:CBIRRE>2.0.CO;2

Creutin, J.D., Delrieu, G., Lebel, T., 1988. Rain Measurement by Raingage-Radar Combination: A Geostatistical Approach. J. Atmospheric Ocean. Technol. 5, 102–115. doi:10.1175/1520-0426(1988)005<0102:RMBRRC>2.0.CO;2

Delrieu, G., Wijbrans, A., Boudevillain, B., Faure, D., Bonnifait, L., Kirstetter, P.-E., 2014. Geostatistical radar–raingauge merging: A novel method for the quantification of rain estimation accuracy. Adv. Water Resour. 71, 110–124. doi:10.1016/j.advwatres.2014.06.005

Ehret, U., 2003. Rainfall and flood nowcasting in small catchments using weather radar. Eigenverlag des Instituts für Wasserbau an der Universität Stuttgart.

Essery, C.I., Wilcock, D.N., 1990. Checks on the measurement of potential evapotranspiration using water balance data and independent measures of

groundwater recharge. J. Hydrol. 120, 51–64. doi:10.1016/0022-1694(90)90141-J

Fang, M., Doviak, R.J., Melnikov, V., 2004. Spectrum Width Measured by WSR-88D: Error Sources and Statistics of Various Weather Phenomena. J. Atmospheric Ocean. Technol. 21, 888–904. doi:10.1175/1520-0426(2004)021<0888:SWMBWE>2.0.CO;2

Fankhauser, R., 1998. Influence of systematic errors from tipping bucket rain gauges on recorded rainfall data. Water Sci. Technol., Use of Historical Rainfall Series for Hydrological ModellingSelected Proceedings of the Third International Workshop on Rainfall in Urban Areas 37, 121–129. doi:10.1016/S0273-1223(98)00324-2

Frederick, R.H., Myers, V.A., Auciello, E.P., 1977. Five to 60 Minute Precipitation Frequency Atlas of the Western United States. NOAA Tech Memo NWS HYDRO-35.

Fulton, R.A., Breidenbach, J.P., Seo, D.-J., Miller, D.A., O'Bannon, T., 1998. The WSR-88D Rainfall Algorithm. Weather Forecast. 13, 377–395. doi:10.1175/1520-0434(1998)013<0377:TWRA>2.0.CO;2

Goovaerts, P., 2000. Geostatistical approaches for incorporating elevation into the spatial interpolation of rainfall. J. Hydrol. 228, 113–129. doi:10.1016/S0022-1694(00)00144-X

Goudenhoofdt, E., Delobbe, L., 2009. Evaluation of radar-gauge merging methods for quantitative precipitation estimates. Hydrol Earth Syst Sci 13, 195–203. doi:10.5194/hess-13-195-2009

Haberlandt, U., 2007. Geostatistical interpolation of hourly precipitation from rain gauges and radar for a large-scale extreme rainfall event. J. Hydrol. 332, 144–157. doi:10.1016/j.jhydrol.2006.06.028

Habib, E., Qin, L., Seo, D.-J., Ciach, G.J., Nelson, B.R., 2013. Independent Assessment of Incremental Complexity in NWS Multisensor Precipitation Estimator Algorithms. J. Hydrol. Eng. 18, 143–155. doi:10.1061/(ASCE)HE.1943-5584.0000638

Heiss, W.H., McGrew, D.L., Sirmans, D., 1990. NEXRAD-Next generation weather radar (WSR-88D). Microw. J. 33, 79.

Jolliffe, I.T., Stephenson, D.B., 2012. Forecast verification: a practitioner's guide in atmospheric science. John Wiley & Sons.

Journel, A.G., 1983. Nonparametric estimation of spatial distributions. J. Int. Assoc. Math. Geol. 15, 445–468. doi:10.1007/BF01031292

Journel, A.G., Huijbregts, C.J., 1978. Mining Geostatistics. Academic Press.

Kim, D., Nelson, B., Seo, D.-J., 2009. Characteristics of Reprocessed Hydrometeorological Automated Data System (HADS) Hourly Precipitation Data. Weather Forecast. 24, 1287–1296. doi:10.1175/2009WAF2222227.1

Krajewski, W.F., 1987. Cokriging radar-rainfall and rain gage data. J. Geophys. Res. Atmospheres 92, 9571–9580. doi:10.1029/JD092iD08p09571

Matheron, G., 1975. Random sets and integral geometry. John Wiley & Sons.

Nelson, B.R., Seo, D.-J., Kim, D., 2010. Multisensor Precipitation Reanalysis. J. Hydrometeorol. 11, 666–682. doi:10.1175/2010JHM1210.1

Schweppe, F.C., 1973. Uncertain dynamic systems. Prentice-Hall.

Seo, D.-J., 2012a. Conditional bias-penalized kriging (CBPK). Stoch. Environ. Res. Risk Assess. 27, 43–58. doi:10.1007/s00477-012-0567-z

Seo, D.-J., 2012b. Conditional bias-penalized kriging (CBPK). Stoch. Environ. Res. Risk Assess. 27, 43–58. doi:10.1007/s00477-012-0567-z

Seo, D.-J., 1998a. Real-time estimation of rainfall fields using radar rainfall and rain gage data. J. Hydrol. 208, 37–52. doi:10.1016/S0022-1694(98)00141-3

Seo, D.-J., 1998b. Real-time estimation of rainfall fields using rain gage data under fractional coverage conditions. J. Hydrol. 208, 25–36. doi:10.1016/S0022-1694(98)00140-1

Seo, D.-J., 1996. Nonlinear estimation of spatial distribution of rainfall — An indicator cokriging approach. Stoch. Hydrol. Hydraul. 10, 127–150. doi:10.1007/BF01581763

Seo, D.-J., Breidenbach, J.P., 2002. Real-Time Correction of Spatially Nonuniform Bias in Radar Rainfall Data Using Rain Gauge Measurements. J. Hydrometeorol. 3, 93–111. doi:10.1175/1525-7541(2002)003<0093:RTCOSN>2.0.CO;2

Seo, D.-J., Krajewski, W.F., Azimi-Zonooz, A., Bowles, D.S., 1990a. Stochastic interpolation of rainfall data from rain gages and radar using Cokriging: 2. Results. Water Resour. Res. 26, 915–924. doi:10.1029/WR026i005p00915

Seo, D.-J., Krajewski, W.F., Bowles, D.S., 1990b. Stochastic interpolation of rainfall data from rain gages and radar using cokriging: 1. Design of experiments. Water Resour. Res. 26, 469–477. doi:10.1029/WR026i003p00469

Seo, D.-J., Siddique, R., Zhang, Y., Kim, D., 2014. Improving real-time estimation of heavy-to-extreme precipitation using rain gauge data via conditional bias-penalized optimal estimation. J. Hydrol. 519, Part B, 1824–1835. doi:10.1016/j.jhydrol.2014.09.055

Seo, D.-J., Smith, J.A., 1996. Characterization of the Climatological Variability of Mean Areal Rainfall Through Fractional Coverage. Water Resour. Res. 32, 2087–2095. doi:10.1029/96WR00486

Sevruk, B., Hertig, J.-A., Spiess, R., 1991. The effect of a precipitation gauge orifice rim on the wind field deformation as investigated in a wind tunnel. Atmospheric Environ. Part Gen. Top. 25, 1173–1179. doi:10.1016/0960-1686(91)90228-Y

Sideris, I.V., Gabella, M., Erdin, R., Germann, U., 2014. Real-time radar–rain-gauge merging using spatio-temporal co-kriging with external drift in the alpine terrain of Switzerland. Q. J. R. Meteorol. Soc. 140, 1097–1111. doi:10.1002/qj.2188

Smith, J.A., Seo, D.J., Baeck, M.L., Hudlow, M.D., 1996. An Intercomparison Study of NEXRAD Precipitation Estimates. Water Resour. Res. 32, 2035–2045. doi:10.1029/96WR00270

Steiner, M., Smith, J.A., Burges, S.J., Alonso, C.V., Darden, R.W., 1999. Effect of bias adjustment and rain gauge data quality control on radar rainfall estimation. Water Resour. Res. 35, 2487–2503.

Vasiloff, S.V., Howard, K.W., Rabin, R.M., Brooks, H.E., Seo, D.-J., Zhang, J., Kitzmiller, D.H., Mullusky, M.G., Krajewski, W.F., Brandes, E.A., Brown, B.G., Berkowitz, D.S., McGinley, J.A., Kuligowski, R.J., 2007. Improving QPE and Very Short Term QPF: An Initiative for a Community-Wide Integrated Approach. Bull. Am. Meteorol. Soc. 88, 1899–1911. doi:10.1175/BAMS-88-12-1899

Velasco-Forero, C.A., Sempere-Torres, D., Cassiraga, E.F., Jaime Gómez-Hernández, J., 2009. A non-parametric automatic blending methodology to estimate rainfall fields from rain gauge and radar data. Adv. Water Resour., Weather Radar and Hydrology 32, 986–1002. doi:10.1016/j.advwatres.2008.10.004

Verworn, A., Haberlandt, U., 2011. Spatial interpolation of hourly rainfall – effect of additional information, variogram inference and storm properties. Hydrol Earth Syst Sci 15, 569–584. doi:10.5194/hess-15-569-2011

Villarini, G., Krajewski, W.F., 2009. Review of the Different Sources of Uncertainty in Single Polarization Radar-Based Estimates of Rainfall. Surv. Geophys. 31, 107–129. doi:10.1007/s10712-009-9079-x

Webster, R., Rivoirard, J., 1991. COPPER AND COBALT DEFICIENCY IN SOIL: A STUDY USING DISJ UN CTIVE KRIGING.

Wilson, J.W., Brandes, E.A., 1979. Radar Measurement of Rainfall—A Summary. Bull. Am. Meteorol. Soc. 60, 1048–1058. doi:10.1175/1520-0477(1979)060<1048:RMORS>2.0.CO;2

Wu, W., Kitzmiller, D., Wu, S., 2011. Evaluation of Radar Precipitation Estimates from the National Mosaic and Multisensor Quantitative Precipitation Estimation System and the WSR-88D Precipitation Processing System over the Conterminous United States. J. Hydrometeorol. 13, 1080–1093. doi:10.1175/JHM-D-11-064.1

Yates, S.R., Warrick, A.W., Myers, D.E., 1986. Disjunctive Kriging: 1. Overview of Estimation and Conditional Probability. Water Resour. Res. 22, 615–621. doi:10.1029/WR022i005p00615

Zhang, J., Howard, K., Langston, C., Vasiloff, S., Kaney, B., Arthur, A., Van Cooten, S., Kelleher, K., Kitzmiller, D., Ding, F., Seo, D.-J., Wells, E., Dempsey, C., 2011. National Mosaic and Multi-Sensor QPE (NMQ) System: Description, Results, and Future Plans. Bull. Am. Meteorol. Soc. 92, 1321–1338. doi:10.1175/2011BAMS-D-11-00047.1

Matheron, G., 1975. Random sets and integral geometry, John Wiley & Sons.

Biographical Information

Beomgeun Kim, who is referred by the name of Ray in America, was born February 1st, 1988 in South Korea. He received the Bachelor of Science in Civil Engineering from Inha University in 2013. He began his Master of Science in water recourses engineering degree in University of Texas at Arlington in 2013. He had the opportunity to work as a graduate research assistant under Dr. Dong Jun Seo of Civil Engineering Department. The author's research interests include radar hydrology, hydrometeorology, groundwater hydrology, and remote sensing.